AD-A274 857

(2)

# NAVAL POSTGRADUATE SCHOOL
## Monterey, California


DTIC
ELECTE
JAN 26 1994
S E D

# THESIS

THE STUDY OF SINGLE-PASS GMA WELDS
WITH DIFFERENT COVER GAS COMPOSITIONS ON
HSLA-100 STEEL

by

Ricky Arthur Seraiva

September, 1993

Thesis Advisor: Alan G. Fox

Approved for public release; distribution is unlimited.

94-02122

94 1 25 019

# REPORT DOCUMENTATION PAGE

Form Approved OMB No. 0704

Public reporting burden for this collection of information is estimated to average 1 hour per response, including the time for reviewing instruction, searching existing data sources, gathering and maintaining the data needed, and completing and reviewing the collection of information. Send comments regarding this burden estimate or any other aspect of this collection of information, including suggestions for reducing this burden, to Washington headquarters Services, Directorate for Information Operations and Reports, 1215 Jefferson Davis Highway, Suite 1204, Arlington, VA 22202-4302, and to the Office of Management and Budget, Paperwork Reduction Project (0704-0188) Washington DC 20503.

| 1. AGENCY USE ONLY | 2. REPORT DATE | 3. REPORT TYPE AND DATES COVERED |
|---|---|---|
| | 23 September 1993 | Master's Thesis |

4. TITLE AND SUBTITLE THE STUDY OF SINGLE-PASS GMA WELDS WITH DIFFERENT COVER GAS COMPOSITIONS ON HSLA-100 STEEL

5. FUNDING NUMBERS

6. AUTHOR(S) *Ricky Arthur Seraiva*

7. PERFORMING ORGANIZATION NAME(S) AND ADDRESS(ES)
Naval Postgraduate School
Monterey, CA 93943-5000

8. PERFORMING ORGANIZATION REPORT NUMBER

9. SPONSORING/MONITORING AGENCY NAME(S) AND ADDRESS(ES)
Naval Surface Warfare Center

10. SPONSORING/MONITORING AGENCY REPORT NUMBER
Code 2814

11. SUPPLEMENTARY NOTES The views expressed in this thesis are those of the author and do not reflect the official policy or position of the Department of Defense or the U.S. Government.

12a. DISTRIBUTION/AVAILABILITY STATEMENT
Approved for public release; distribution is unlimited.

12b. DISTRIBUTION CODE

13.

ABSTRACT The purpose of this study was to investigate the effect of varying cover gas compositions on the microstructure and mechanical properties of single run gas-metal arc welds (GMAW) on HSLA-100 plate and seven different cover gas compositions containing varying amounts of argon, oxygen, and carbon dioxide were evaluated. A statistical and quantitative analysis of the nonmetallic inclusions in the welds metal was performed by scanning electron microscopy (SEM) and energy dispersive analysis of x_rays (EDX). These results showed that increasing the oxygen content of the cover gas reduced the inclusion size but increases the number density compared with pure argon cover gas, and that this was reflected in the weld metal microstructure since increasing amounts of acicular ferrite were detected predominantly to be of the spessartite composition ($3MnO$, $Al_2O_3$, $3SiO_2$). As a result of increasing cover gas oxygen the strength of the weld metal appeared to be lowered due to the oxidation of aluminum, silicon, manganese, and possibly titanium. In addition, the toughness was improved for weld metal generated from cover gases containing oxygen because the ductile-to -brittle transition temperature was lowered by the increasing amounts of acicular ferrite.

14. SUBJECT TERMS GMAW, HSLA-100, NONMETALLIC INCLUSIONS, SPESSARTITE, ACICULAR FERRITE

15. NUMBER OF PAGES 73

16. PRICE CODE

| 17. SECURITY CLASSIFICATION OF REPORT | 18. SECURITY CLASSIFICATION OF THIS PAGE | 19. SECURITY CLASSIFICATION OF ABSTRACT | 20. LIMITATION OF ABSTRACT |
|---|---|---|---|
| Unclassified | Unclassified | Unclassified | UL |

NSN 7540-01-280-5500

Standard Form 298 (Rev. 2-89)
Prescribed by ANSI STD. 239-18

Approved for public release; distribution is unlimited.

# THE STUDY OF GMA WELDS WITH DIFFERENT COVER GAS COMPOSITIONS ON HSLA-100 STEEL

by

Ricky Arthur Seraiva
Lieutenant , United States Navy
B.S., Temple University

Submitted in partial fulfillment
of the requirements for the degree of

MASTER OF SCIENCE IN MECHANICAL ENGINEERING

from the

NAVAL POSTGRADUATE SCHOOL
September 1993

Author: Ricky Arthur Seraiva

Ricky Arthur Seraiva

Approved by: Alan G. Fox

Alan G. Fox, Thesis Advisor

Matthew Kelleher

Matthew D. Kelleher, Chairman
Department of Mechanical Engineering

## ABSTRACT

The purpose of this study was to investigate the effect of varying cover gas composition on the microstructure and mechanical properties of single run gas-metal arc welds (GMAW) on HSLA-100 plate and seven different cover gas compositions containing varying amounts of argon, oxygen, and carbon dioxide. A statistical and quantitative analysis of the nonmetallic inclusions in the weld metal was performed by scanning electron microscopy (SEM) and energy dispersive analysis of x-rays (EDX). These results showed that increasing the oxygen content of the cover gas reduced the inclusion size but increased the number density compared with pure argon cover gas, and that this was reflected in the weld metal microstructure since increasing amounts of acicular ferrite were detected as oxygen was added. The composition of these inclusions was found predominantly to be of the spessartite composition ($3MnO$, $Al_2O_3$, $3SiO_2$). As a result of increasing cover gas oxygen the strength of the weld metal appeared to be lowered due to the oxidation of aluminum, silicon, manganese, and possibly titanium. In addition, the toughness was improved for weld metal generated from cover gases containing oxygen because the ductile-to-brittle transition temperature was lowered by the increasing amounts of acicular ferrite.



DTIC QUALITY INSPECTED 5





| Accesion For | |
|---|---|
| NTIS CRA&I | X |
| DTIC TAB | ☐ |
| Unannounced | ☐ |
| Justification | |
| By | |
| Distribution / | |
| Availability Codes | |
| Dist | Avail and / or Special |
| A-1 | |

## TABLE OF CONTENTS

## LIST OF TABLES

## LIST OF FIGURES

## ACKNOWLEDGMENT

I would like to thank the faculty and staff of the Mechanical Engineering Department, with special thanks to Dr. Alan Fox for their patience, guidance, and support in completing this research.

For their support, guidance, and love I would like to thank my wife Jeannie and son Robert. They always seem to understand that it took endless hours at the lab to complete the research.

I would also like to thank my parents, who provided me with a strong backbone, that made it possible to keep the pursuit going when times got tough.

# I. INTRODUCTION

In order to reduce construction costs in its shipbuilding interest, the U.S. Navy has been investigating the certification of high strength low alloy (HSLA) 100 steels, to replace high yield (HY) 100 steels. HY steels, because of their carbon content and carbon equivalent, require complicated welding procedures. These include strict control of pre-heat, interpass, and post-heating temperatures to avoid hydrogen embrittlement and cracking. HSLA steels, because of their lower carbon content, permit welding under less stringent heat input and temperature controls. This allows for a generous reduction in man-hour cost during the structural fabrication of HSLA steels vice HY steels. Current efforts towards the certification of HSLA-100 steels with HY-100 welding consumable have yielded adequate results. These results indicated that the distribution and composition of non-metallic inclusion within the fusion zone play a important role in the overall strength and toughness of a weldment.

Gas metal arc welding (GMAW) is a welding process that uses a gas cover atmosphere over the molten weld pool to exclude the oxidizing effects of air. In consideration of arc stability and cost effectiveness, small quantities of ionized oxygen or carbon dioxide are added with the effect of stabilizing the arc and reducing weld splatter. Argon and

oxygen or carbon dioxide are added with the effect of stabilizing the arc and reducing weld splatter. Argon and mixes of argon with carbon dioxide (90% Ar-10% $CO_2$) or argon with oxygen (90% Ar-4% $O_2$) are typically used in the welding of HSLA steels.

The focus of this study is to examine the size, frequency, distribution and composition of non-metallic inclusions in gas metal arc welds on HSLA-100 steels, as a function of shield gas composition and to investigate the effect these inclusions have on weld metal strength and toughness. The goal of this research is to optimise cover gas compositions for GMAW.

# II. BACKGROUND

## A. CHARACTERISTICS OF HSLA-100 STEELS

High strength low alloy (HSLA) steels are low carbon, copper precipitation strengthened steels. The strengthening mechanisms utilized in HSLA steels include grain refinement, precipitation strengthening and solid solution strengthening. The strength and toughness of HSLA steels is dependent on the small grains produced during the thermomechanical processing. To achieve the higher strengths and toughness required in ship structures, though, precipitation of copper through overaging is also required. Successful microalloying in HSLA-100 steel development is the key to this steel's excellent mechanical properties. Alloy additions effect every strengthening mechanism in steel with the exception of mechanical processing.

The chemical composition for HSLA-100 steel is listed in Table 1 (pg. 22). The metallurgical effects of each of these alloys are listed below:

- Carbon - The function of carbon is to make the steel stronger, harder and wear resistant. This is done by it's ability to form martensite which increases strength. Carbon also has the ability to be an excellent solid solution strengthener. The extremely low carbon content of HSLA-100 steels contributes to better weldability, lowers the susceptibility to hydrogen cracking and lower ductile to brittle transition temperature (DBTT). (Czyryca, 1990)

- Manganese - Reacts with sulfur to form MnS, preventing the formation of harmful FeS at grain boundaries which cause 'hot cracking'. Manganese has the tendency to lower the critical temperature point; therefore, the steel can be hardened at a lower temperature. (Hertzburg, 1989)

- Silicon - One of the most important applications of silicon is its use as a deoxidizer in molten steel. Silicon increases hardening ability and strengthens steel. Silicon decreases the solubility of carbon in iron, which results in a stronger steel with less carbon. Manganese, chromium and molybdenum are added with silicon to give a deep hardening effect. (Ellis, 1990)

- Nickel - Increases strength by enhancing grain refinement and solid solution strengthening. Nickel has little effect on the hardening ability of steel, but adds to the toughness and wear resistance. (Wilson, 1988)

- Niobium - Combines with nitrogen and carbon to form niobium carbon nitride, which provide grain refinement during hot rolling and later austenitizing treatment by pinning the austenite grain boundaries. Increases strength through carbide and nitride formation. (Wilson, 1988)

- Chromium - Essentially chromium is a hardening agent. Like manganese, chromium causes the hardness to penetrate deeper, therefore enhancing the wear properties of the steel. Chromium is a strong carbide former. (Wilson, 1988)

- Copper - Increases strength by precipitation of copper-rich particles during aging. Improves corrosion resistance to seawater and reduces susceptibility to hydrogen induced cracking. (Wilson, 1988)

- Molybdenum - Added to steel to improve the heat-treatment properties. Molybdenum increases the hardening penetration and when used in conjunction with silicon, manganese, or chromium this element increase strength. (Wilson, 1988)

- Vanadium - Is one of the strong carbide-forming elements. It dissolves to some degree in ferrite, impairing strength and toughness. (Hertzburg, 1989)

- Titanium - Precipitates of carbide on nitride, may serve as nucleation sites for acicular ferrite. Titanium containing inclusion have been identified as being

particularly effective in the nucleation of intergranular acicular ferrite. (Mattes, 1990)

- Aluminum - An effective deoxidizing agent and refines the grain structure of the weld metal through the formation of aluminum nitride which pin grain boundaries and inhibit grain growth. (Porter, 1982)

The percentage of an alloy element required for its given purpose range from .02 to 4.0 weight percent. The only way that an alloying element can affect the properties of the steel is to change the dispersion of carbides in the ferrite, change the property of the ferrite, or change the properties of the carbide. The effect on the distribution of carbide is the most important factor. In large sections where carbon steels will fail to harden throughout the section, the hardenability of the steel can be increased by the addition of an alloying element. Increases in hardenability permit the hardening of a larger section of alloy steel over carbon steel and a reduction or elimination of the quenching operation. Consequently there are lower smaller thermal stresses, which will reduce cracking or warping. The elements most effective in increasing the hardenability of steel are manganese, silicon, chromium, molybdenum, copper, and niobium. (Suka,1992)

Elements such as molybdenum, tungsten, chromium, and vanadium are used for increasing the hardness when dissolved in austenite, but these are often present in the form of carbides. They can also reduce the agglomeration of carbide

in tempered martensite. This is the main advantage of carbide-forming elements. Tempering relieves the internal stresses in hardened steel and cause spherordization of the carbide particles with resultant loss in hardness and strength. The presence of these stable-carbide forming elements enable higher temperatures to be used without a loss in strength. This imparts to these alloys steels the character of greater ductility for a given strength, or conversely greater strength for a given ductility, than plain carbon steels. (Suka, 1992)

The presence of alloying elements in the ferrite is the key to contributions of greater strength. Any element in solid solution in iron will increase its strength. The most effective elements for imparting greater strength have been formed to be phosphorous, manganese, nickel, silicon, tungsten, and chromium.

The alloys also influence the austenitic grain size. Martensite formed from a fine-grain austenite has considerably greater resistance to shock then when formed from coarse grain austenite. The oxides formed by the deoxidation of the steel by different elements apparently prevent grain growth above the critical temperature over a considerable temperature range. To inhibit grain-growth, the most elective element is aluminum. A similar effect on the austenite grain size results from the presence of finely scattered carbide in the austenite. Elements forming stable carbides and nitrides will

also contribute to the formation of a fine-grained austenite. In HSLA-100 niobium carbonitride precipitates effect such control. (Macks, 1958)

The use of copper as an alloying element in low carbon HSLA steel has resulted in the following improvements; increased strength through precipitation of copper (while retaining toughness), greater weldability and formability, excellent corrosion resistance, high fatigue strength and resistance to fatigue crack growth, and suppression of hydrogen-induced cracking. The negative effect of added copper is the increased potential for hot shortness during hot working. (Winters, 1991)

## B. GAS METAL ARC WELDING (GMAW)

Gas metal arc welding (MIG) is a gas shielded metal-arc welding process which uses the high heat of an electric arc between a continuously fed, consumable electrode wire and the material to be welded. Metal is transferred through the gas protected arc column to the work.

In this process, a wire is fed continuously from a reel through a gun to a contact surface which imparts a current to the wire. A fixed relationship exists between the rate of wire burn-off and the welding current. This means at a fixed wire feed speed rate, the welding machine will produce the current necessary to maintain the arc. The welding current, which is indicated on the machine ammeter ranges from 100 to

400 amps, depending on the size of the consumable wire. (Kuo,1987)

Solid bare wires in size from .035" to .125" diameter are usually used and should have mechanical properties similar to the base metal, if the strength of the weldment is to be close to that of the base plate, as is required by some U.S. Navy standards.

The welding gun can be either air or water cooled depending upon the amperage being used. Continuous high amperage work is performed with a water cooled gun.

The purpose of the shielded gas is to displace the atmosphere around the weld pool. This will help eliminate contamination of the weld metal while it solidifies.

There are three basic types of metal transfer modes; globular, spray transfer, and short-circuiting in the GMAW process (Kuo,1987). Generally, globular transfer is desired for flat, downward directed welds because it produces the least splatter and is fast. Spray transfer is preferred for overhead because the molten metal can be directed upward under the influence of the arc force. Short-circuiting is the mode that produces a lot of splatter and is best used in the flat position moving toward the welder. (Kuo, 1987)

## C. WELD ZONE TOUGHNESS

The weld metal composition is the resultant effect of the base metal, welding wire and cover gas composition. Some of

the more easily oxidized elements will react and either accumulate on the weld pool surface as slag or provide a site for nucleation of a inclusion in the weld metal. The inclusion shape, size, and distribution will effect metallurgical transformation nucleation rates. Since the mechanical properties of the weld fusion zone are dependent of the microstructure, any parameter which influences the fusion zone microstructure will also influence the strength and toughness of the weld. Thus, any changes in power density, welding speed, or gas composition will have an influence on the microstructure, which will affect the mechanical properties of the weldment. Such changes in these variables can lead to changes in both strength and toughness. For example, cover gases which contain oxygen can lead to oxidation of manganese, aluminum, and silicon and to a loss of strength. The same oxygen can also generate large numbers of small oxide inclusions which can nucleate acicular ferrite and improve toughness by lowering the ductile-to-brittle-transition temperature (DBTT). (Kuo, 1987)

This acicular ferrite is a fine microstructure that is randomly orientated with short ferrite needles that have a basketweave structure. This basketweave structure resists propagation of a fracture by presenting a very irregular fracture path. Therefore, frequent directional changes are necessary for fracture. The formation of either grain boundary ferrite, side plate ferrite or the needles of the

bainite with their high aspect ratio, alternatively offer long straight crack propagation paths. In addition, the long ferrite needles can be bounded by a layers of brittle carbide, which forms as a result of the reduction of carbon solubility in iron when cooled from the austenite stability range to the ferrite stability range. (Kuo, 1987)

Two primary changes occur in the fusion zone microstructure due to changes in welding parameters, which result in alteration of the cooling rate. First, a slower cooling rate will generally produce coarser microstructural features. Second, change of the cooling rates will influence the nucleation and growth processes involved in the decomposition of austenite into proeutectiod ferrite, eutectoidal ferrite plus carbide or martensite. (Kuo,1987)

## D. EFFECTS OF COVER GAS COMPOSITION

Another factor that can influence the microstructure of the HSLA weldments is the cover gas oxygen activity. Oxygen composition variations do not have a linear relationship to the chemical reactions involved in welding. In order for the relationship to be linear, an ideal solution would have to be present. Very dilute solutions may approach an ideal situation. The deviation from ideal is accounted for by establishing the relationship between the free energy of a component in the solution and a coefficient that takes place

on the mole fraction of the component. This term is referred to as the chemical activity and is expressed by the formula:

$$F=RT \ln A$$

F= molar free energy

R= universal gas constant

T= absolute temperature

A= chemical activity

Changes in oxygen activity will result in changes in the amount of weld metal constituents which are oxidized. This, in turn, will result in a change in composition, morphology, size, and quantity of oxide particles formed in the weld metal fusion zone, as mentioned previously. (Francis, 1987)

The part that oxides play in the formation of acicular ferrite has yet to be totally understood. It is clear that some relationship exists between the presence of oxides and nitride particles and the nucleation of acicular ferrite but it appears to be rather complex. It is not clear what type of oxide is required for the nucleation of acicular ferrite. Various combinations of size, shape, distribution, composition, thermal expansion coefficient, and surface energy have been considered with no apparent outcome. A generous trend seems to be that an increase of acicular ferrite occurs as oxygen content increases but only to a point, after which the amount of acicular ferrite begins to decrease (Francis,1984).

Two opposite effects can be defined due to oxide changes. First, some of these oxides will act as nucleation sites and promote the decomposition of austenite into ferrite upon cooling. The behavior is easily understood as a shift to the left of the curves in a CCT diagram, figure 1 (pg. 23). The other effect involves a change in the manganese content of the oxides. As the oxide content changes with increasing metal oxygen content, the oxide particle which is produced is richer in silicon dioxide and less rich in manganese oxide (Francis, 1987). The resulting matrix chemistry can also shift, increasing the soluble manganese and the hardening ability of the weld. In general, solid oxides tend to stay as small and separate particles. The liquid oxides can more easily cluster and grow, thereby reducing the number of nucleation sites. In addition, being lighter than the molten metal, the larger agglomerated liquid oxides of the manganese-silicon mixed types will more easily rise to the surface, separating from the weld pool, and be withdrawn as possible nucleation sites. (Francis, 1984)

## III. EXPERIMENT

Seven different automated bead on plate welds were made with the only variable being the cover gas composition of the gas metal arc weld process. The welding parameters were 28 volts, 260 amps, travel speed of 9 inches per minute, heat input of 43.6 kilojoules per inch, and shielding gas flow rate of 50 cubic feet per hour. The shielding gas composition in weight percent for each weld were as follows; 100% argon, 98% argon-2% $O_2$ (M-2), 96% argon-4% $O_2$ (M-4), 95% argon-5% $CO_2$ (C-5), 90% argon-10% $CO_2$ (C-10), 50% C-10-50% M-4, and 33% C-10 33% M-4-33% argon (figure 2). The automated gas metal arc welds were made on a one inch base plate of HSLA-100 steel, whose composition is listed in Table 2. The 140-S, 1/16" diameter electrode composition is listed in Table 2, and was stored in a heated cabinet before use. The base plate was sandblasted and cleaned with acetone before welding at ambient temperature.

These welds are to be examined in order to try and determine the composition, non-metallic inclusion characteristics and mechanical properties (on multi-run versions). To try and understand the effect of cover gas composition on weld metal strength and toughness.

## IV. EXAMINATION PROCEDURE

The experimental procedure consist of three distinct operations. First, a statistical and quantitative analysis was performed on the scanning electron microscope (SEM) to determine the size of the inclusions. Second, a quantitative analysis of the inclusion compositions was made through the energy dispersive x-ray (EDX) and analysis. Third, the specimens were etched for a qualitative analysis through optical and electron microscopy. The welds to be examined were sectioned in the transverse direction. The welds were surface ground, hand sanded (240, 320, 400, and 600 grits), then polished up to one micron using diamond paste.

In order to complete the first step, the secondary electron (SE) mode on the SEM was used to investigate the size of the inclusions. Due to the small size of the inclusions, the SEM was operated at a working distance of 8 mm and 4000x magnification. One hundred fields of view were randomly examined and recorded for each sample. Each field of view represented an area of 500 micrometers$^2$. The diameter of every inclusion per field was recorded. The measurement was made by using the two cursors on the SEM and logging the separation distance between the lines.

To determine the inclusion composition, the magnification of each inclusion was increased up to 40,000 times with the working distance at 16 mm in the SE mode. The x-ray spectrum for each inclusion was examined by using the spot scan controls. The analysis was terminated after 140,000 counts were achieved. This spectrum was then saved on the Kevex software. The average size of an inclusion was 0.7 microns. As the x-ray analyzer has a bulb of interaction that is about 2 microns in diameter the base matrix spectrum has to be removed. A second x-ray spectrum ,therefore, has to be made of a inclusion-free weld metal. The Kevex was then used to subtract the background matrix from the inclusion matrix, leaving a x-ray spectrum showing the elements present in the inclusion. The inclusion spectrum is then analyzed to determine the composition of the inclusion.

The third step in the examination procedure was to use optical microscopy to determine the microstructure of the weld. All seven specimens were etched for approximately 5-10 seconds in a 5% nital solution. The etched surfaces were examined at various magnifications using a Zeiss ICM 405 microscope.

# V. RESULTS AND DISCUSSION

## A. INCLUSION QUANTITY, SIZE, AND COMPOSITION

One hundred fields of view for each specimen were examined on the SEM. Each field of view represented 500 micrometers$^2$. Figure 3 represents a typical etched field in the weld metal. The inclusion are all very dark and spherical. The size ranged from .2 micron up to 3.5 microns in diameter. Figure 4-10 represent the frequency distribution for the inclusion diameters for each gas metal arc weld. A statistical analysis was performed on the data and Table 3 represents the number of inclusions, mean, standard deviation minimum and maximum for each weld. Table 4 represents the inclusion area density and the total inclusion area per field.

The statistical data supports evidence that there is direct correlation between quantity and size of inclusions to the percent oxygen in the cover gas. Figure 11 is a graph showing how the number of inclusions increase as percent oxygen in the cover gas increases. Figure 12 is a graph showing how inclusion diameter decreases as percent oxygen in the cover gas increases.

Oxygen in the arc atmosphere can affect the weld metal in three different ways: oxidizing alloying elements, porosity, and precipitation of non-metallic inclusions. The weld pool

is formed as droplets of weld metal fall from the electrode to the base metal. Each droplet is surrounded by the cover gas and has a high surface/volume ratio. In the hot spot of the weld pool just below the arc, temperatures are estimated to be greater than 2000 degrees centigrade. The high temperature along with the weld pool stirring allows for large amounts of oxygen to dissolve. Silicon and manganese do not seem to act as deoxidants at temperatures greater than 1800 degrees centigrade (Lancaster,1987). Figure 13 shows the results of the increase in weld metal oxygen as percent cover gas oxygen increases. Figures 14-17 represent the decrease of silicon, manganese, aluminum, and titanium as percent oxygen in the cover gas increases. Tables 5 and 6 are the weld metal composition (weight percent) provided by Naval Surface Warfare Center.

Tables 7-13 represent the oxide composition of twenty inclusions for each weld. The last row in each table represents the average composition for that table. The results of the averages appear on Table 14. The composition for the oxides are fairly constant. The ratio appears not to change with cover gas oxygen. The reduction in size of the inclusion appears to be directed at the oxidation of silicon, manganese, aluminum and titanium, figures 14-17, as percent cover gas oxygen increases. The quantity of inclusion must be directly related to the oxidation of a supersaturated liquid as it proceeds towards equilibrium. Figure 18 represents how

the quantity of inclusions relates to the size of the inclusions.

Figure 19 is a schematic representation of the $MnO-SiO_2-Al_2O_3$ system. Titanium is omitted from the phase determination for two reasons. First, there is a relatively small quantity involved. Second, there is also the possibility the titanium is present as the nitride, TiN, which forms first and acts as a nucleant for the oxide portion of the inclusion. Eighty percent of the inclusion plot around the homogeneity range of Spessartite. The chemical formula for spessartite is $3MnO + Al_2O_3 + 3SiO_2$ with a stoichiometric composition in weight percent of 43% MnO, 36% $SiO_2$, and 21% $Al_2O_3$.

To summarize, five effects were observed. Weld metal oxygen increases as cover gas oxygen increases. Weld metal silicon, manganese, aluminum, and titanium decrease as cover gas oxygen increase. The average inclusion diameter decreases as cover gas oxygen increases. The number of inclusion per field increase as cover gas oxygen increases. The composition of the inclusion appears to be similar to spessartite (figure 19), if titanium is omitted.

## B. MICROSTRUCTURE

The microstructure depends primarily on two major items which affect the nucleation and growth processes: cooling rates and weld metal compositions. The cooling rate is a function of the heat input, pre-heat, voltage, current, travel

speed, and arc efficiencies. The weld compositions are a function of the base plate metal, weld wire metal and cover gas. Examining a temperature versus log-time plot diagram for a particular composition, it is evident that a slow cooling rate will produce a blocky proeutectoid grain boundary ferrite as part of the austenite decomposition product (Francis, 1987). A faster cooling rate can produce a microstructure predominately of acicular ferrite. Still faster cooling rates will produce bainite.

Figure 20, 21, and 22 are photographs of the etched weldments magnified 400 times. This represents the three corners of the ternary cover gas diagram. Figure 20, 100% argon cover gas represents a 100% bainite/martensite structure throughout. M2 cover gas weld displayed a significant amount of acicular ferrite and bainite. It appears that acicular ferrite content increases with oxygen in the cover gas, figures 21 and 22. This is difficult to quantify because as the percent oxygen in the cover gas increases the grain structure gets finer. The difference in the amount of acicular ferrite between the welds that have oxygen in the cover gas appears to be minor.

## C. MECHANICAL PROPERTIES

Since the microstructure of all the welds are bainite-like, the following equation was used to calculate the tensile strength (Pickering, 1978):

$$T.S.\ (MN/m^2) = 15.4[16 + 125(C) + 15(Mn + Cr) + 12(Mo) + 6(W) + 8(Ni) + 4(Cu) + 25\ (V + Ti)]$$

The results are graphed on figure 23. The results of the graph demonstrate that the loss of the weld metals (Al, Si, Mn, and Ti) due to oxidation have a direct loss on the tensile strength.

The Charpy impact results supplied from by the Naval Surface Warfare Center are plotted on figure 24. These results are for multipass welds which demonstrate an increase in toughness for the $-60^0F$ curve as cover gas oxygen increases. This is directly related to the increase in acicular ferrite, since its presence has apparently lowered the DBTT.

Figure 25 represents the hardness for the M2 and M4 cover gas. Figure 26 represents the hardness for C5, midpoint, C10/M4 and C10 cover gas. These tables were separated to show how carbon from carbon dioxide and carbon monoxide affects the hardness by:

$$2CO_2 = 2CO + O_2$$

$$2CO = 2C + O_2$$

As can be seen from these chemical reaction equations, carbon is a product which can cause an increase in the carbon content of the weld metal, or at least, prevent carbon losses.

## VI. SUMMARY

The following is a list of conclusions developed from this thesis:

- The average inclusion diameter decreases as cover gas oxygen increases.
- The number of inclusions increase as cover gas oxygen increases.
- Weld metal oxygen increases as cover gas oxygen increases.
- Weld metal silicon, aluminum, manganese, and titanium decrease as cover gas oxygen increases.
- Weld metal oxide inclusion compositions do not vary significantly with cover gas oxygen.
- The oxide inclusion compositions are similar to the homogeneity range of spessartite.
- The weld metal microstructure for 100% argon cover gas is bainite/martensite.
- The weld metal microstructure for cover gas with oxygen consist of bainite and acicular ferrite.
- The amount of acicular ferrite in the weld metal appears to increase as cover gas oxygen increases.
- Weld metal tensile strengths appear to decrease due to losses of alloying elements from oxidation, when cover gases with oxygen and carbon dioxide are used.
- There is an improvement in weld metal impact toughness as cover gas oxygen increases as increasing amounts of acicular ferrite shifts the DBTT to lower temperatures.
- Weld metal hardness decreases only for M2 and M4 cover gases which contain oxygen rather than just $CO_2$. This is no doubt due to the oxidizing effect of pure $O_2$ which are almost certainly greater than $CO_2$ because of increases oxygen activity. This almost certainly leads to carbon losses when oxygen is used.

TABLE 1. HSLA-100 STEEL MIL-S-24645A COMPOSITION

(weight percent)

| | |
|---|---|
| Carbon | 0.040-0.060 |
| Manganese | 0.750-1.050 |
| Phosphorous | 0.020 |
| Sulfur | 0.006 |
| Silicon | 0.400 |
| Nickel | 3.350-3.650 |
| Chromium | 0.450-0.750 |
| Molybdenum | 0.550-0.650 |
| Copper | 1.450-1.750 |
| Niobium | 0.020-0.060 |

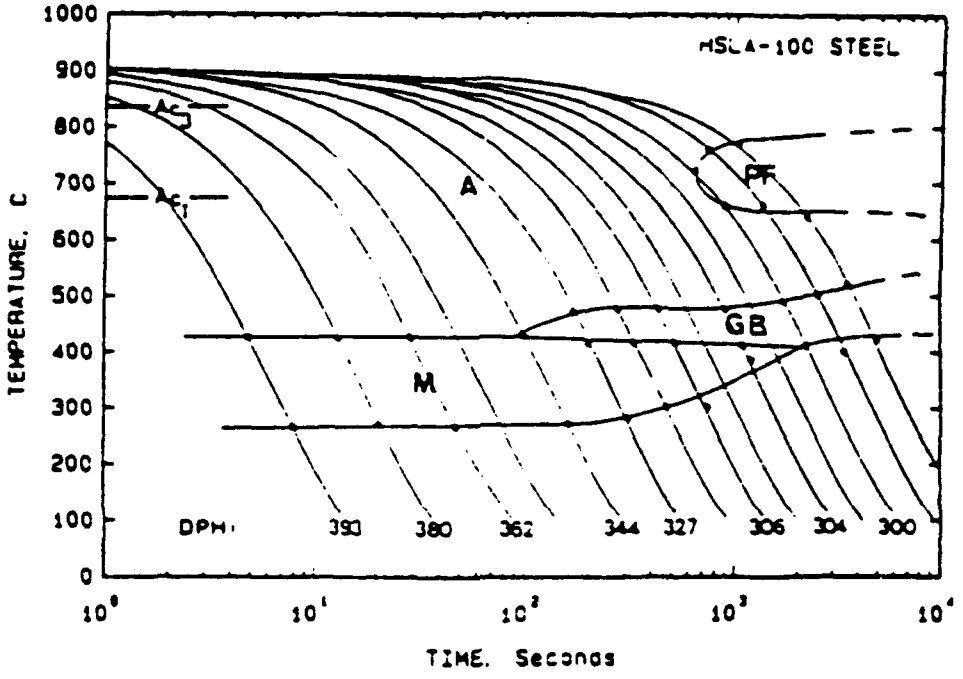


Figure 1. HSLA-100 Steel Continous Cooling Transformation Diagram. (Wilson, 1988)

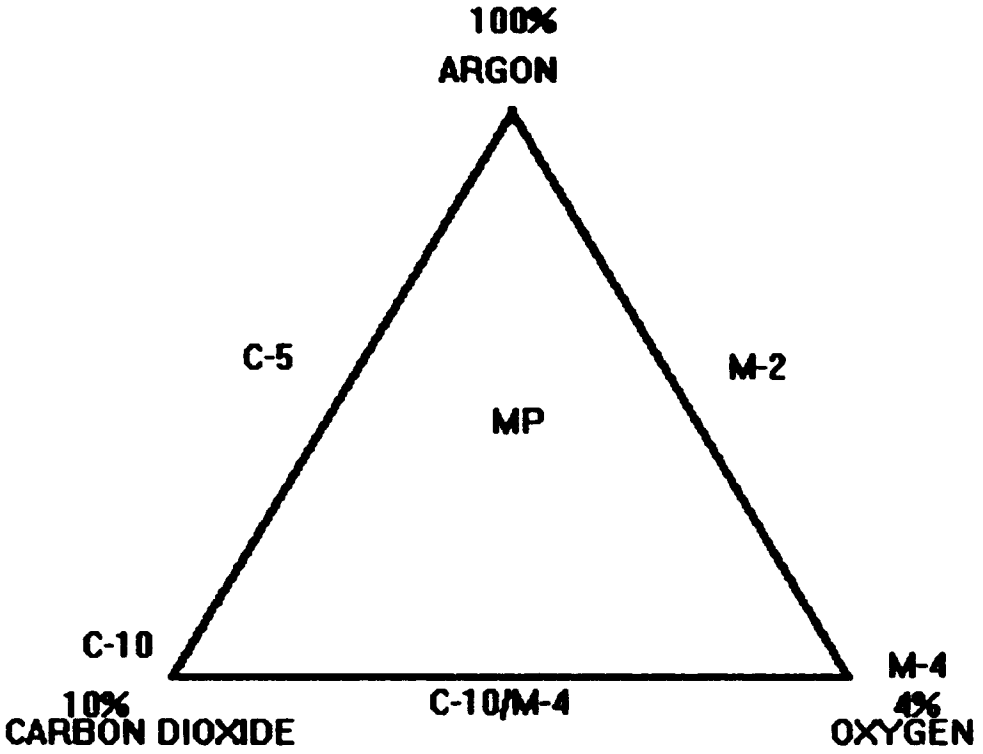


Figure 2. Diagram of the simplex design used for shielding gas compositions.

TABLE 2. WEIGHT PERCENT COMPOSITION FOR HSLA 100 STEEL AND 140-S ELECTRODE

| | BASE PLATE AVG. | WELD WIRE AVG. |
|---|---|---|
| CARBON | .075 | .079 |
| MANGANESE | .793 | 1.518 |
| SILICON | .365 | .428 |
| PHOSPHOROUS | .010 | .005 |
| SULFUR | 0.000 | .002 |
| NICKEL | 3.307 | 2.518 |
| MOLYBDENUM | .587 | .852 |
| CHROMIUM | .543 | .746 |
| NIOBIUM | .024 | 0.000 |
| VANADIUM | .003 | .003 |
| ALUMINUM | .020 | .007 |
| TITANIUM | .004 | .016 |
| ZIRCONIUM | 0.000 | .005 |
| COPPER | 1.633 | .034 |
| OXYGEN | .002 | .014 |
| NITROGEN | .011 | .004 |
| BORON | .003 | .004 |
| HYDROGEN | .300 | 0.000 |

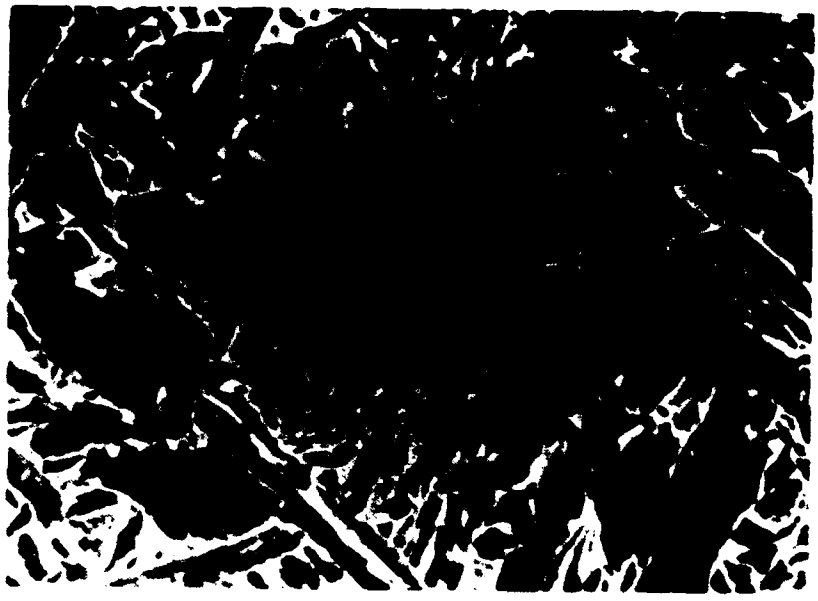

Figure 3. SEM micrograph of gas metal arc weld on HSLA-100 steel. (4000x, 8mm working distance)

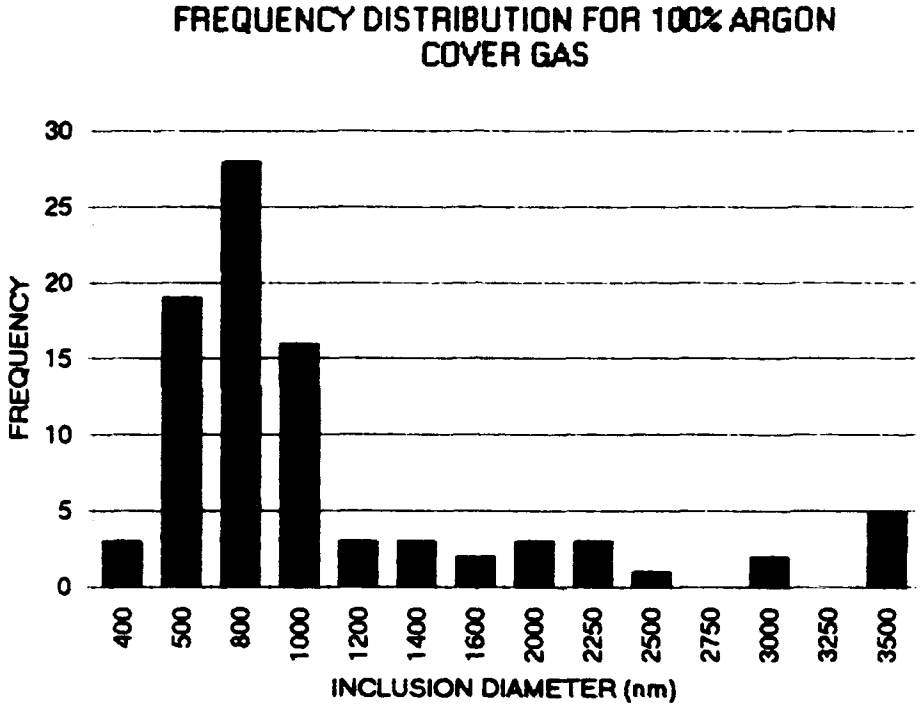


Figure 4. Bar chart representing the number of inclusions versus the diameter of the inclusion for 100 % Argon cover gas.

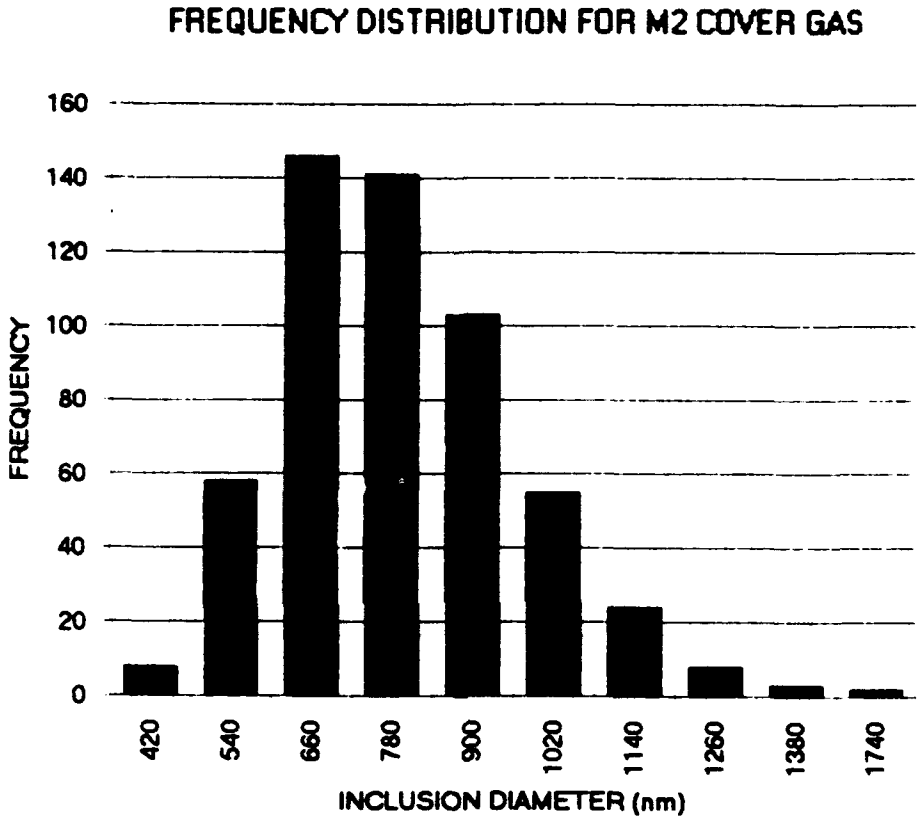


Figure 5. Bar chart representing the number of inclusions versus the diameter of the inclusion for M2 cover gas.

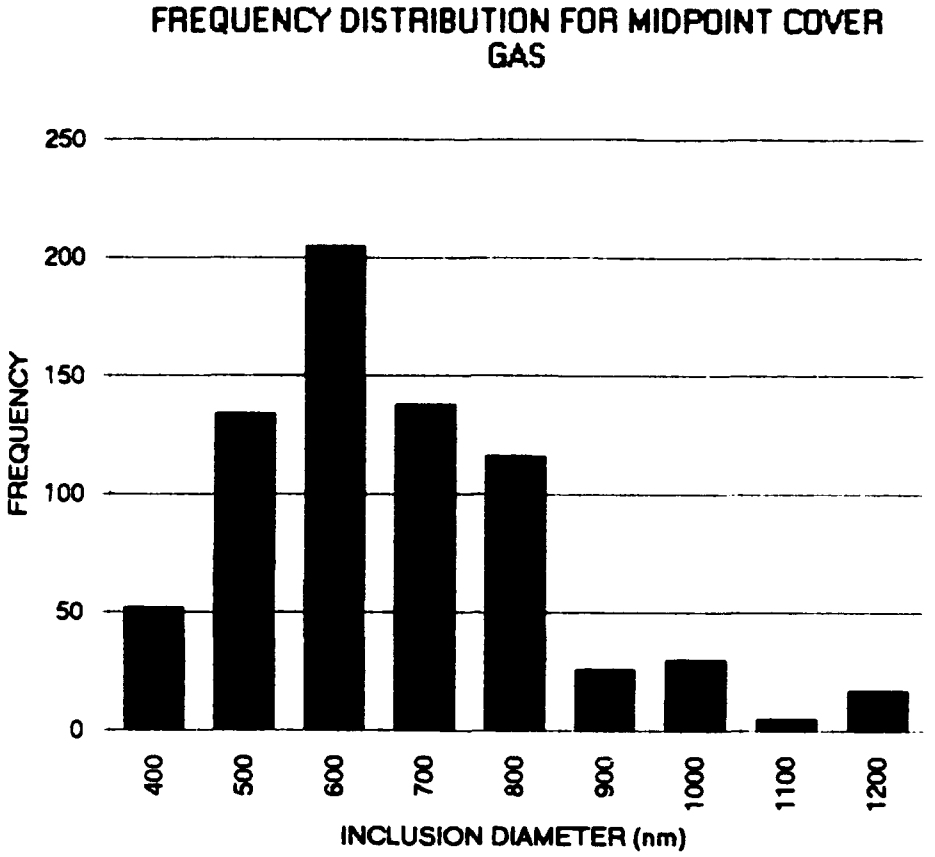


Figure 6. Bar chart representing the number of inclusions versus the diameter of the inclusion for midpoint cover gas.

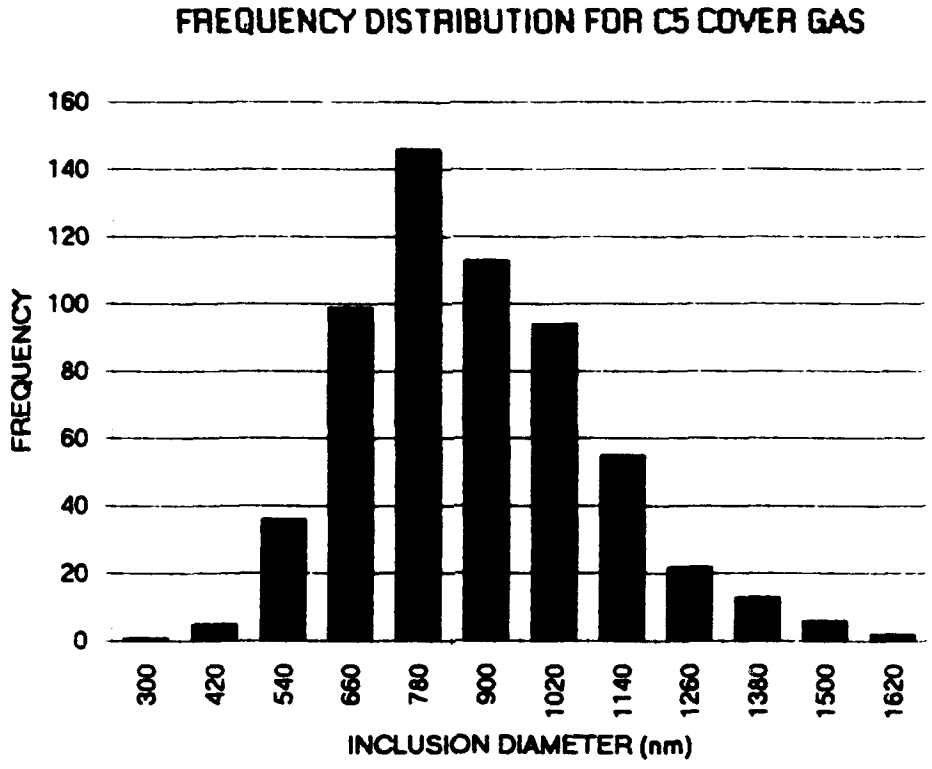


Figure 7. Bar chart representing the number of inclusions versus the diameter of the inclusion for C5 cover gas.

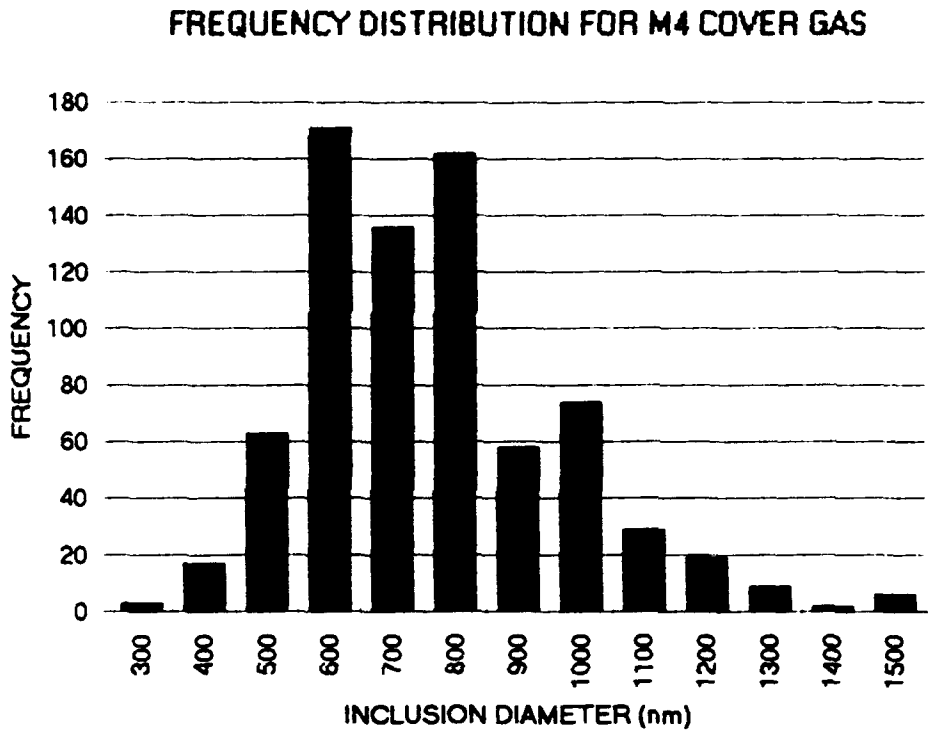


Figure 8. Bar chart representing the number of inclusions versus the diameter of the inclusion for M4 cover gas.

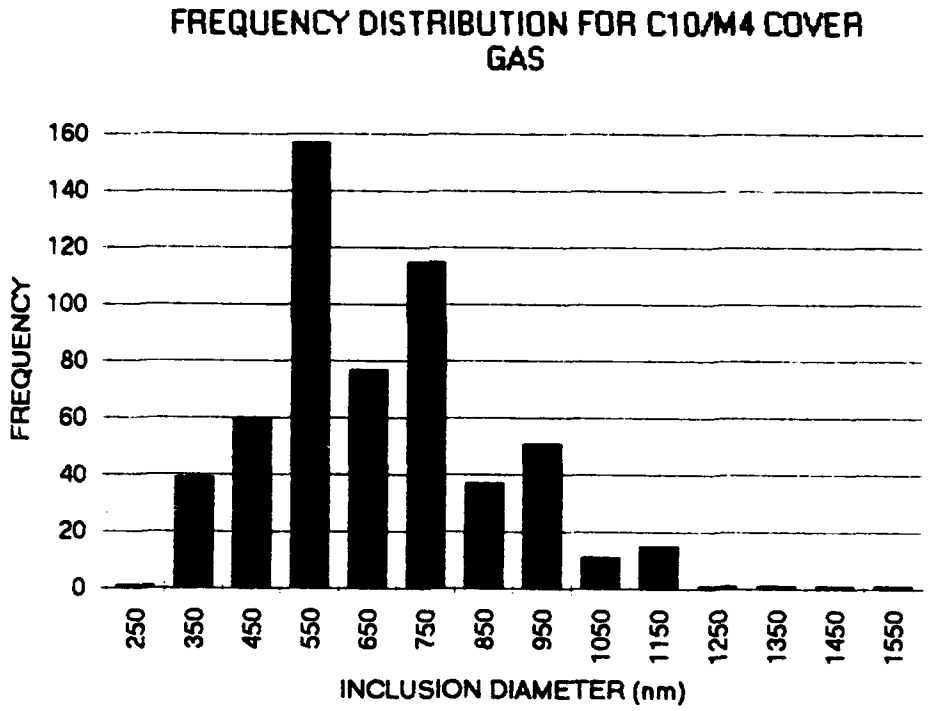


Figure 9. Bar chart representing the number of inclusions versus the diameter of the inclusion for C10/M4 cover gas.

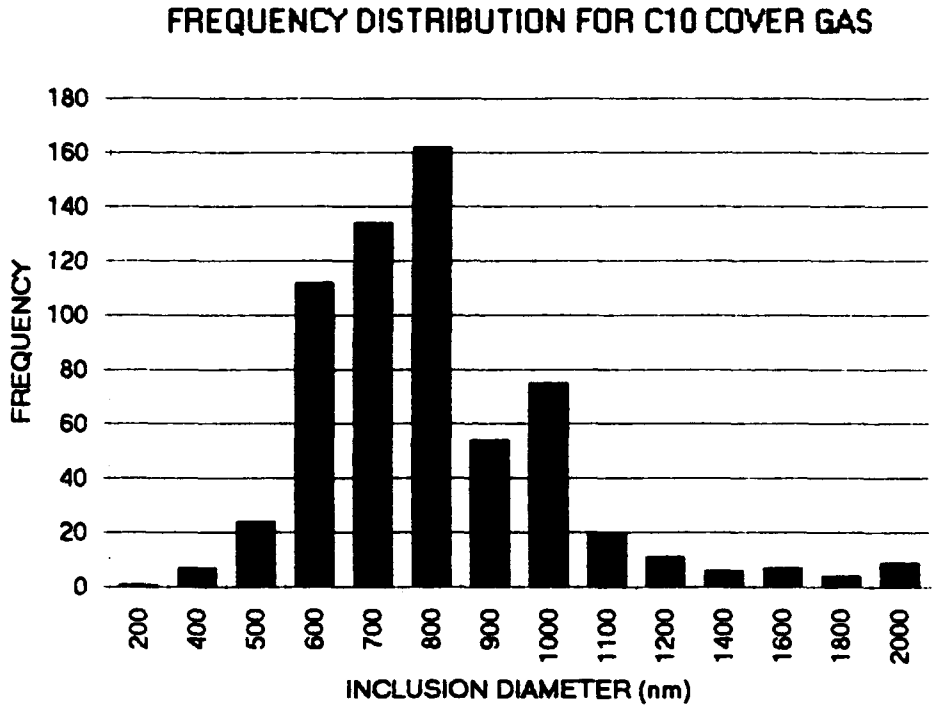


Figure 10. Bar chart representing the number of inclusion versus the diameter of the inclusion for C10 cover gas.

TABLE 3. FREQUENCY TABLE FOR EACH WELD

| N | MEAN SIZE (nm) | STANDARD DEVIATION | MIN. | MAX. | COVER GAS |
|---|---|---|---|---|---|
| 88 | 1294 | 1467 | 451 | 9800 | 100 Ar |
| 548 | 800 | 173 | 400 | 1760 | M2 |
| 723 | 668 | 206 | 320 | 3010 | MIDPOINT |
| 592 | 879 | 202 | 309 | 1670 | C5 |
| 749 | 765 | 218 | 121 | 2670 | M4 |
| 567 | 667 | 193 | 251 | 1560 | C10/M4 |
| 626 | 821 | 330 | 121 | 5290 | C10 |

TABLE 4. INCLUSION AREA DENSITY AND INCLUSION AREA PER FIELD

| AREA DENSITY INCLUSION/$U^2$ X $10^4$ | INCLUSION AREA PER FIELD U/FIELD X $10^{-6}$ | COVER GAS |
|---|---|---|
| .176 | .995 | 100% Ar |
| 1.10 | 2.75 | M2 |
| 1.44 | 2.53 | MIDPOINT |
| 1.18 | 3.59 | C5 |
| 1.50 | 3.44 | M4 |
| 1.13 | 1.98 | C10/M4 |
| 1.25 | 3.31 | C10 |

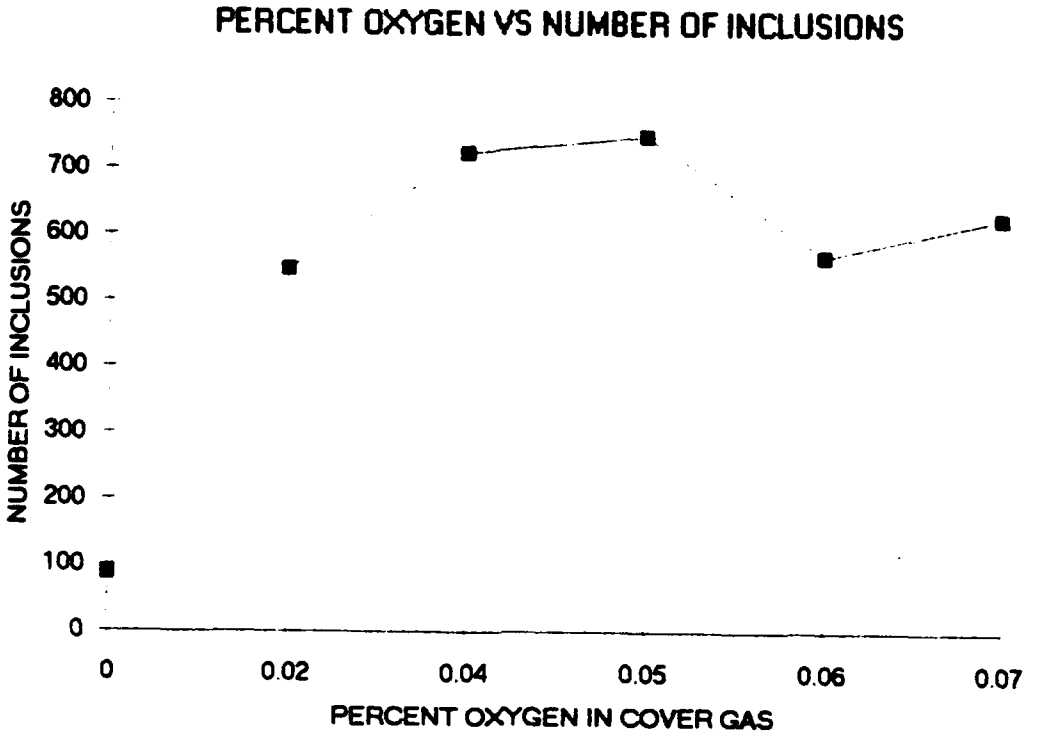


Figure 11. Line chart representing the increase in the number of inclusions versus cover gas oxygen.

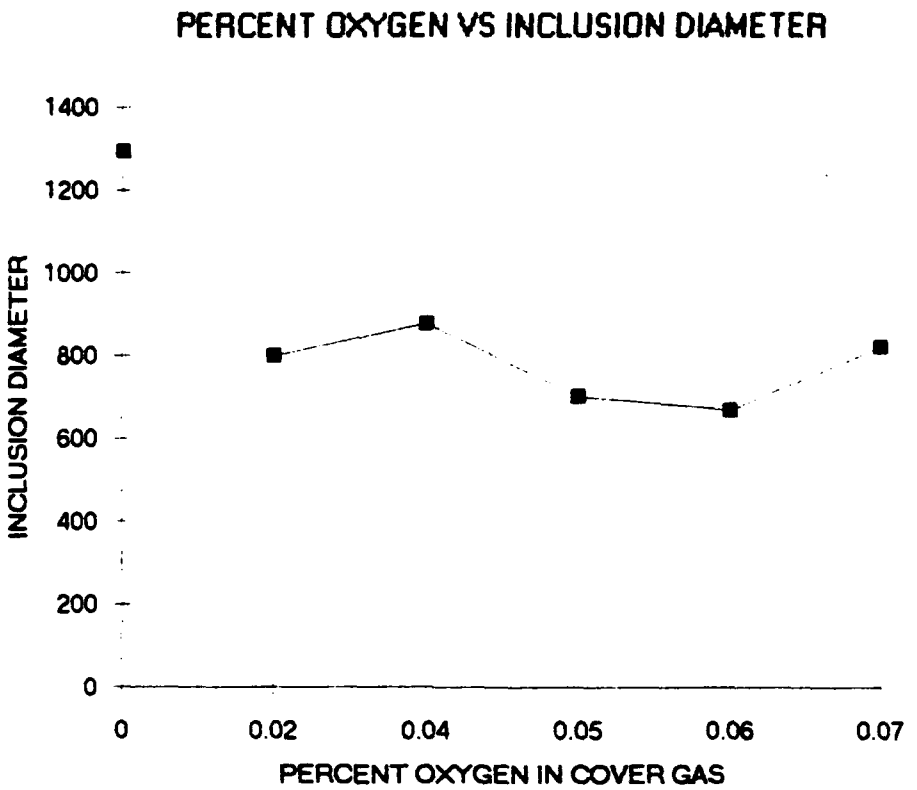


Figure 12. Line chart representing the decrease in inclusion diameter versus cover gas oxygen.

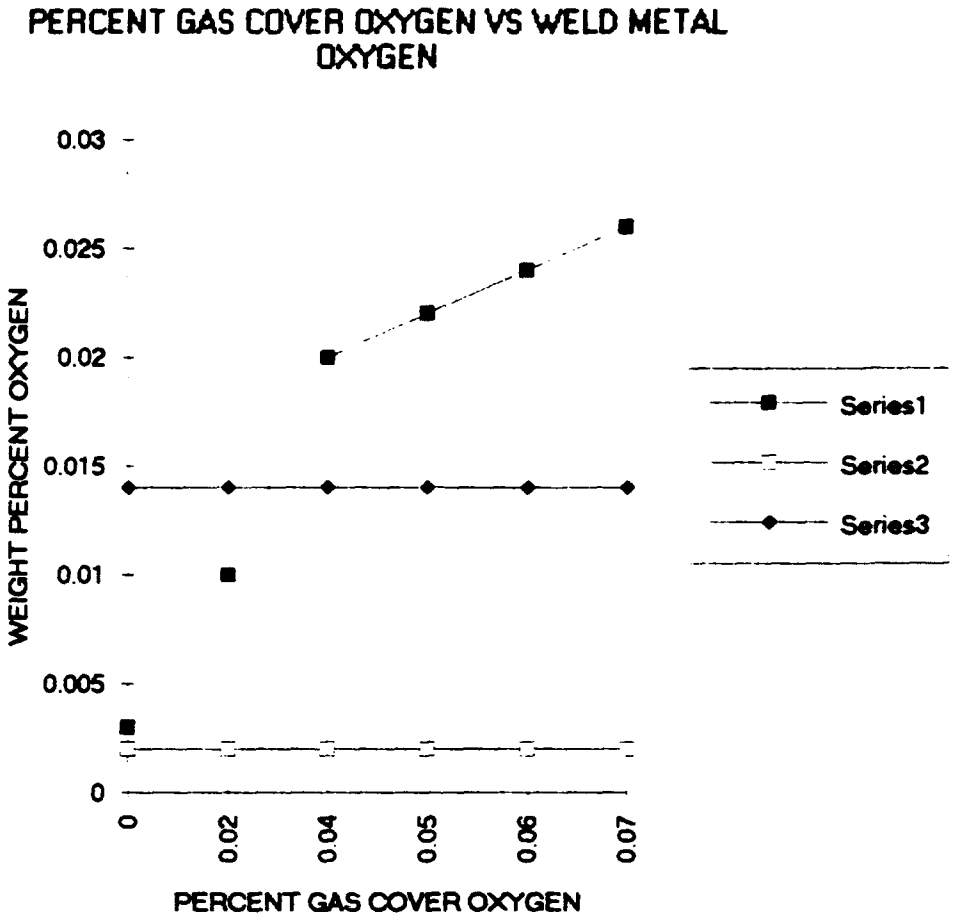


Figure 13. Line chart representing the increase in weld metal oxygen versus cover gas oxygen.Series 1,2, and 3 represent the weld metal, base plate and electrode composition respectively.

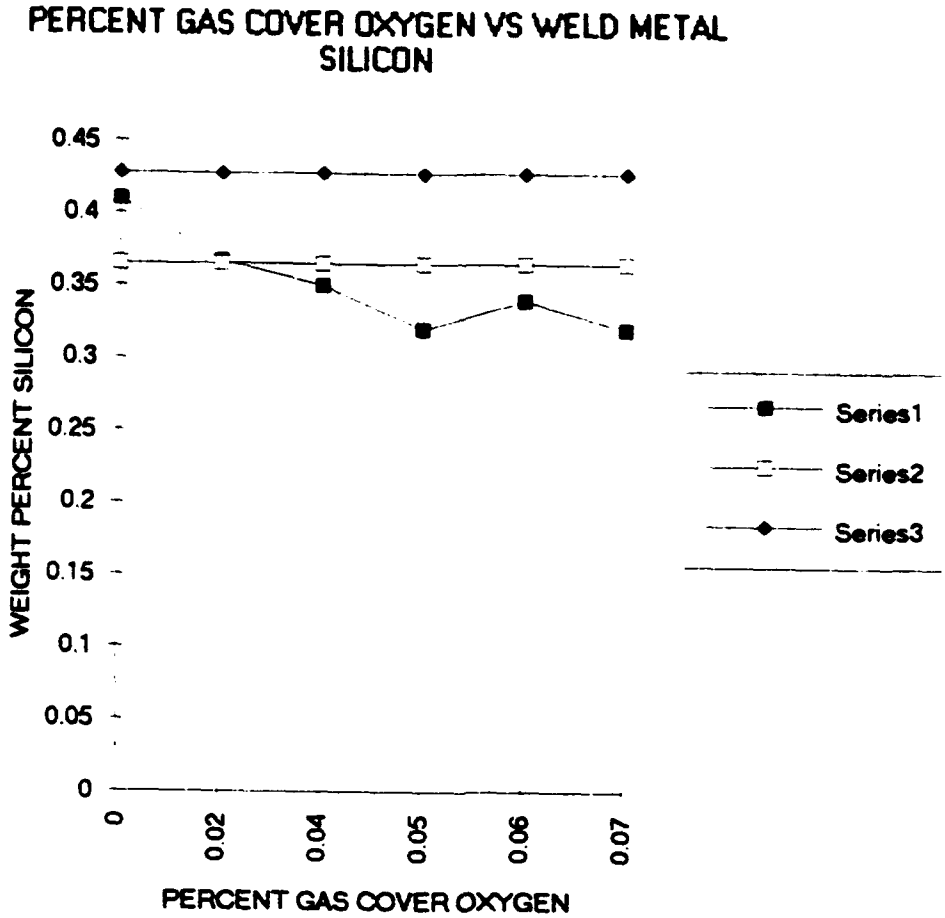


Figure 14. Line chart representing the decrease in weld metal silicon versus cover gas oxygen. Series 1,2,and 3 represent the weld metal, base plate and electrode compositions respectively.

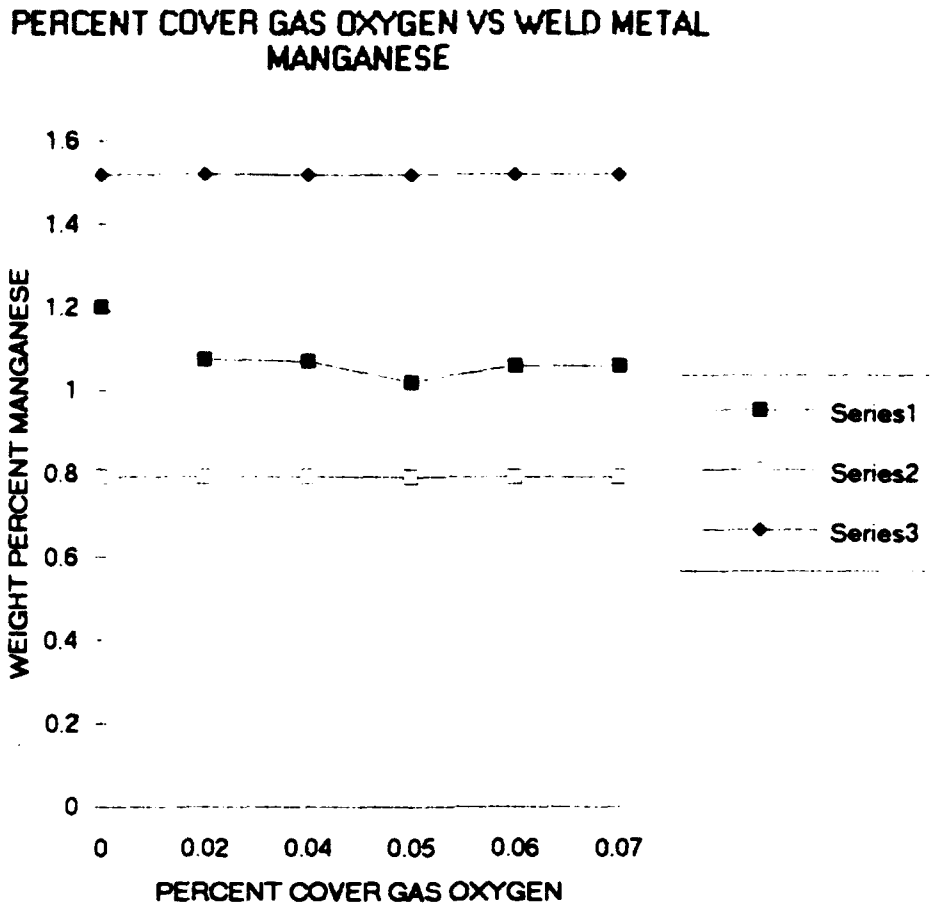


Figure 15. Line chart representing the decrease in weld metal manganese versus cover gas oxygen. Series 1, 2, and 3 represent the weld metal, base plate, and electrode compositions respectively.

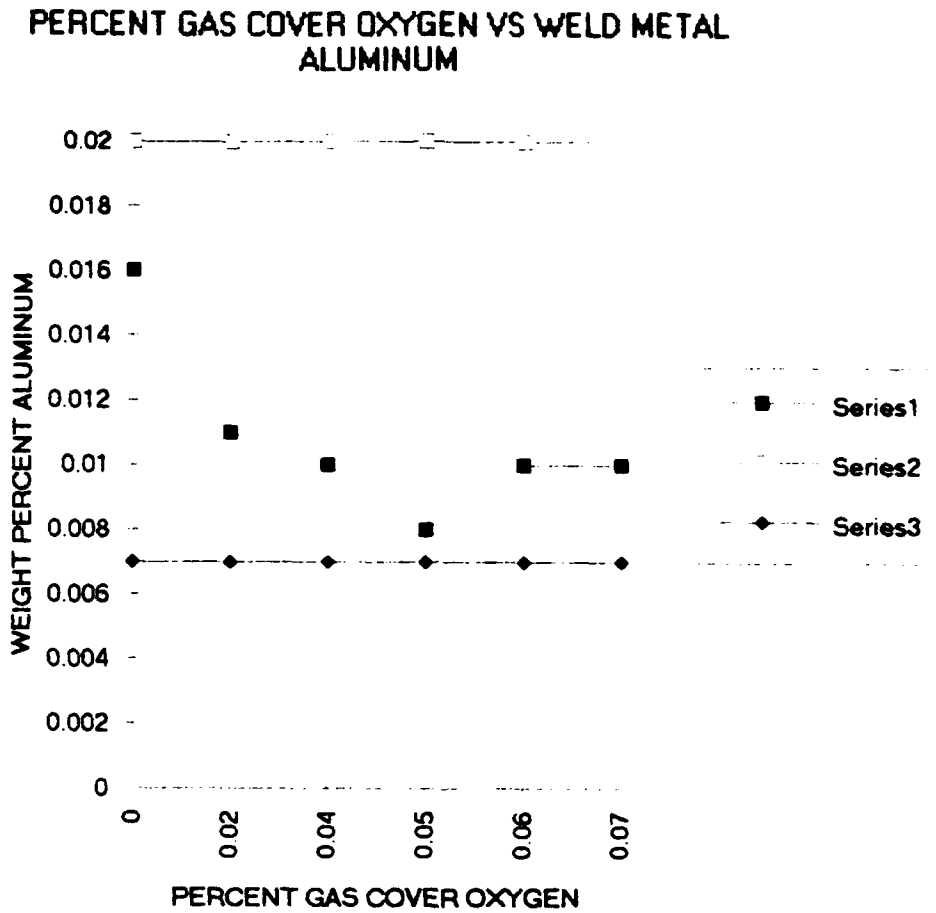


Figure 16. Line chart representing the decrease in weld metal aluminum versus cover gas oxygen. Series 1, 2, and 3 represent the weld metal, base plate, and electrode compositions respectively.

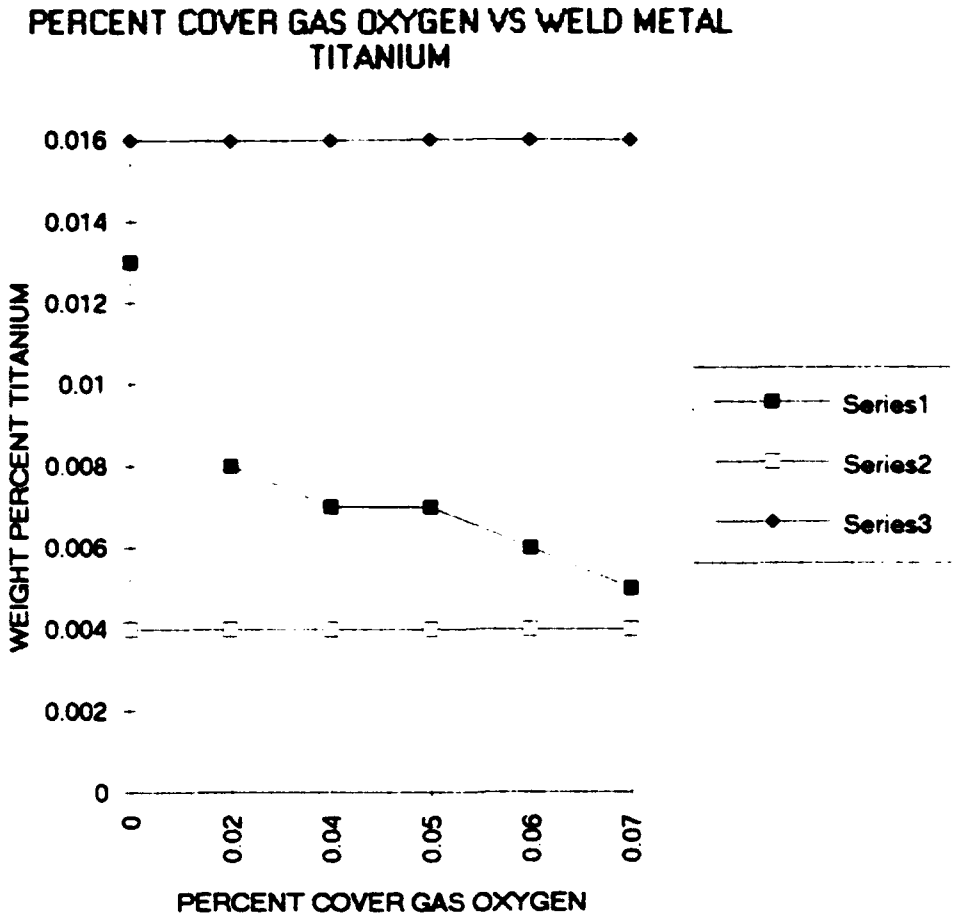


Figure 17. Line chart representing the decrease in weld metal titanium versus cover gas oxygen. Series 1, 2, and 3 represent the weld metal, base plate, and electrode compositions respectively.

TABLE 5. WELD METAL COMPOSITIONS
(weight percent)

| COVER GAS | C10 | C5 | MID POINT |
|---|---|---|---|
| CARBON | .069 | .069 | .070 |
| MANGANESE | 1.000 | 1.070 | .0701 |
| SILICON | .320 | .340 | .360 |
| PHOSPHORUS | .008 | .006 | .007 |
| SULFUR | <.001 | <.001 | <.002 |
| NICKEL | 2.930 | 2.840 | 2.780 |
| MOLYBDENUM | .730 | .767 | .757 |
| CHROMIUM | .660 | .680 | .700 |
| NIOBIUM | .016 | .015 | .015 |
| VANADIUM | .003 | .003 | .003 |
| ALUMINUM | .0103 | .009 | .011 |
| TITANIUM | .005 | .007 | .008 |
| ZIRCONIUM | <.001 | <.001 | <.001 |
| COPPER | .907 | .703 | .717 |
| OXYGEN | .026 | .026 | .019 |
| NITROGEN | .097 | .008 | .008 |
| BORON | .0042 | .005 | .004 |
| HYDROGEN PPM | .330 | .400 | .400 |

TABLE 6. WELD METAL COMPOSITIONS
(weight percent)

| COVER GAS | M2 | M4 | C10/ M4 | 100% Ar |
|---|---|---|---|---|
| CARBON | .065 | .067 | .064 | .069 |
| MANGANESE | 1.073 | 1.020 | 1.060 | 1.200 |
| SILICON | .367 | .320 | .347 | .410 |
| PHOSPHOROUS | .007 | .009 | .005 | .008 |
| SULFUR | .002 | .001 | .001 | .001 |
| NICKEL | 2.700 | 2.740 | 2.870 | 2.880 |
| MOLYBDENUM | .723 | .750 | .730 | .810 |
| CHROMIUM | .640 | .647 | .680 | .720 |
| NIOBIUM | .014 | .014 | .015 | .015 |
| VANADIUM | .003 | .003 | .003 | .003 |
| ALUMINUM | .011 | .008 | .010 | .016 |
| TITANIUM | .008 | .007 | .006 | .013 |
| ZIRCONIUM | .001 | .001 | .001 | .001 |
| COPPER | .710 | .663 | .773 | .693 |
| OXYGEN | .020 | .025 | .024 | .003 |
| NITROGEN | .008 | .007 | .008 | .006 |
| BORON | .005 | .004 | .005 | .004 |
| HYDROGEN PPM | .400 | .330 | .370 | .400 |

TABLE 7. OXIDE COMPOSITIONS PRESENT IN GMAW WITH 100% ARGON COVER GAS

| ALUMINUM | SILICON | TITANIUM | MANGANESE | OXYGEN |
|---|---|---|---|---|
| 0.00 | 0.00 | 9.07 | 65.73 | 25.20 |
| 15.02 | 15.02 | 12.36 | 14.63 | 42.98 |
| 20.75 | 8.34 | 4.54 | 27.40 | 38.97 |
| 15.28 | 5.42 | 2.78 | 42.51 | 34.00 |
| 22.23 | 0.00 | 3.44 | 40.48 | 33.86 |
| 21.07 | 9.99 | 6.97 | 21.07 | 40.91 |
| 17.51 | 0.00 | 7.70 | 41.88 | 32.91 |
| 15.19 | 15.19 | 11.49 | 15.19 | 42.93 |
| 15.28 | 20.28 | 0.92 | 20.28 | 43.23 |
| 16.94 | 0.00 | 18.32 | 28.99 | 35.75 |
| 1.34 | 44.91 | 0.28 | 0.70 | 52.76 |
| 18.05 | 18.05 | 2.38 | 18.05 | 43.47 |
| 6.99 | 7.06 | 5.34 | 48.61 | 31.99 |
| 0.43 | 46.01 | 0.43 | 0.04 | 53.09 |
| 8.66 | 23.39 | 1.76 | 23.80 | 42.42 |
| 9.53 | 0.00 | 10.56 | 49.86 | 30.05 |
| 17.74 | 17.74 | 12.94 | 5.39 | 46.20 |
| 0.00 | 3.06 | 9.30 | 60.37 | 27.28 |
| 0.29 | 46.12 | 0.32 | 0.19 | 53.08 |
| 0.00 | 0.00 | 14.08 | 59.26 | 26.66 |
| 12.77 | 19.32 | 6.68 | 30.14 | 38.56 |

Note: Last line represents the average for that column.

TABLE 8. OXIDE COMPOSITIONS PRESENT IN GMAW WITH M2 COVER GAS

| ALUMINUM | SILICON | TITANIUM | MANGANESE | OXYGEN |
|---|---|---|---|---|
| 13.39 | 15.40 | 13.10 | 15.40 | 42.70 |
| 11.11 | 20.40 | 5.40 | 20.41 | 42.68 |
| 4.59 | 20.72 | 43.95 | 0.00 | 30.73 |
| 8.80 | 17.75 | 13.18 | 16.14 | 42.13 |
| 12.04 | 16.74 | 11.84 | 16.60 | 42.58 |
| 16.72 | 18.33 | 3.31 | 16.33 | 43.31 |
| 11.70 | 19.39 | 6.81 | 19.40 | 42.70 |
| 12.05 | 19.64 | 5.91 | 19.64 | 42.76 |
| 16.04 | 17.61 | 5.58 | 17.61 | 43.17 |
| 11.23 | 14.71 | 0.00 | 39.84 | 34.22 |
| 12.33 | 18.26 | 8.44 | 16.26 | 42.72 |
| 8.31 | 13.64 | 16.75 | 21.05 | 40.25 |
| 12.55 | 15.06 | 14.73 | 15.06 | 42.57 |
| 13.30 | 17.15 | 9.61 | 17.05 | 42.79 |
| 10.94 | 16.36 | 13.86 | 16.38 | 42.43 |
| 12.60 | 16.97 | 10.77 | 16.97 | 42.68 |
| 11.93 | 15.66 | 14.24 | 15.66 | 42.52 |
| 11.72 | 15.68 | 14.42 | 15.68 | 42.49 |
| 17.50 | 17.55 | 4.04 | 17.55 | 43.37 |
| 12.04 | 17.21 | 11.99 | 18.50 | 41.50 |

Note: Last line represents the average for that column.

TABLE 9. OXIDE COMPOSITIONS PRESENT IN GMAW WITH MIDPOINT COVER GAS

| ALUMINUM | SILICON | TITANIUM | MANGANESE | OXIDE |
|---|---|---|---|---|
| 5.71 | 8.27 | 4.04 | 50.17 | 31.81 |
| 14.31 | 14.31 | 14.31 | 14.31 | 42.76 |
| 14.12 | 15.93 | 11.19 | 15.93 | 42.83 |
| 11.48 | 18.65 | 8.59 | 18.65 | 42.63 |
| 13.73 | 16.27 | 10.94 | 16.27 | 42.79 |
| 15.51 | 15.52 | 10.46 | 15.52 | 42.99 |
| 10.21 | 14.61 | 10.18 | 25.15 | 39.85 |
| 0.00 | 16.13 | 2.44 | 47.57 | 33.86 |
| 8.93 | 21.86 | 4.87 | 21.87 | 42.47 |
| 0.00 | 25.11 | 8.16 | 25.29 | 41.43 |
| 7.70 | 20.09 | 9.08 | 21.16 | 41.97 |
| 7.07 | 7.53 | 7.46 | 44.95 | 32.96 |
| 12.20 | 19.25 | 6.54 | 19.25 | 42.75 |
| 13.02 | 18.62 | 6.11 | 19.66 | 42.60 |
| 12.55 | 20.35 | 3.88 | 20.35 | 42.87 |
| 10.57 | 20.80 | 5.19 | 20.80 | 42.63 |
| 10.21 | 19.06 | 9.13 | 19.09 | 42.48 |
| 16.65 | 19.98 | 0.00 | 19.98 | 43.39 |
| 15.10 | 20.83 | 0.00 | 20.83 | 43.23 |
| 11.71 | 17.53 | 7.80 | 24.04 | 40.96 |

Note: Last line represents the average for that column.

TABLE 10. OXIDE COMPOSITIONS PRESENT IN GMAW WITH C5 COVER GAS

| ALUMINUM | SILICON | TITANIUM | MANGANESE | OXYGEN |
|---|---|---|---|---|
| 9.27 | 11.36 | 16.11 | 24.25 | 39.01 |
| 9.36 | 19.96 | 8.24 | 20.00 | 42.42 |
| 17.05 | 17.05 | 5.56 | 17.05 | 43.28 |
| 10.18 | 19.93 | 7.42 | 19.93 | 42.53 |
| 10.08 | 17.71 | 12.11 | 17.71 | 42.39 |
| 12.63 | 17.77 | 9.10 | 17.77 | 42.73 |
| 12.85 | 17.42 | 9.56 | 17.42 | 42.74 |
| 11.89 | 19.06 | 7.29 | 19.06 | 42.71 |
| 9.47 | 18.45 | 11.24 | 18.46 | 42.34 |
| 8.56 | 19.11 | 10.90 | 19.13 | 42.27 |
| 8.70 | 17.32 | 13.60 | 18.46 | 41.93 |
| 11.99 | 17.77 | 9.82 | 17.77 | 42.65 |
| 9.77 | 19.69 | 8.21 | 19.92 | 42.41 |
| 8.99 | 19.64 | 9.36 | 19.66 | 42.35 |
| 12.76 | 19.38 | 5.63 | 19.38 | 42.84 |
| 16.64 | 17.39 | 5.33 | 17.39 | 43.24 |
| 9.07 | 21.44 | 5.57 | 21.45 | 43.24 |
| 10.72 | 18.68 | 9.38 | 16.66 | 42.47 |
| 15.29 | 16.30 | 9.11 | 16.30 | 42.33 |
| 15.67 | 17.74 | 5.71 | 17.74 | 43.00 |
| 11.55 | 18.16 | 8.94 | 18.77 | 42.44 |

Note: Last line represents the average for that column.

TABLE 11. OXIDE COMPOSITIONS PRESENT IN GMAW WITH M4 COVER GAS

| ALUMINUM | SILICON | TITANIUM | MANGANESE | OXYGEN |
|---|---|---|---|---|
| 16.32 | 16.33 | 7.89 | 16.33 | 43.14 |
| 17.12 | 17.98 | 3.58 | 17.96 | 43.34 |
| 11.07 | 18.46 | 9.41 | 18.46 | 42.56 |
| 13.69 | 16.63 | 6.14 | 18.63 | 42.92 |
| 17.66 | 17.66 | 3.64 | 17.66 | 43.39 |
| 14.68 | 17.04 | 8.28 | 17.04 | 43.96 |
| 10.62 | 9.10 | 14.64 | 27.93 | 37.72 |
| 16.08 | 16.13 | 8.56 | 16.13 | 43.10 |
| 17.00 | 17.06 | 5.61 | 17.06 | 43.27 |
| 17.28 | 14.49 | 7.47 | 18.50 | 42.26 |
| 16.77 | 19.92 | 0.00 | 19.92 | 43.40 |
| 13.63 | 19.10 | 5.23 | 19.10 | 43.94 |
| 18.72 | 18.64 | 0.00 | 18.84 | 43.60 |
| 14.85 | 18.77 | 4.53 | 18.77 | 43.08 |
| 23.36 | 0.00 | 15.40 | 23.37 | 37.87 |
| 18.80 | 18.80 | 0.00 | 18.80 | 43.61 |
| 0.00 | 22.96 | 12.73 | 22.96 | 41.35 |
| 4.19 | 41.58 | 1.26 | 0.80 | 52.17 |
| 0.00 | 3.07 | 17.56 | 49.65 | 29.70 |
| 18.77 | 18.81 | 0.00 | 18.81 | 43.61 |
| 15.59 | 18.03 | 8.25 | 19.84 | 42.30 |

Note: Last line represents the average for that column.

TABLE 12. OXIDES COMPOSITIONS PRESENT IN GMAW WITH C10/M4 COVER GAS

| ALUMINUM | SILICON | TITANIUM | MANGANESE | OXYGEN |
|---|---|---|---|---|
| 15.07 | 16.45 | 4.93 | 18.45 | 43.09 |
| 9.71 | 16.17 | 15.67 | 16.19 | 42.25 |
| 16.72 | 16.72 | 6.63 | 16.72 | 43.21 |
| 14.66 | 17.30 | 7.77 | 17.30 | 42.90 |
| 12.48 | 16.63 | 11.61 | 16.63 | 42.65 |
| 11.32 | 20.72 | 4.51 | 20.72 | 42.72 |
| 10.50 | 19.50 | 7.35 | 19.51 | 42.54 |
| 13.00 | 17.25 | 9.75 | 17.25 | 42.75 |
| 17.30 | 17.30 | 4.77 | 17.30 | 43.32 |
| 9.50 | 20.65 | 6.72 | 20.65 | 42.48 |
| 11.72 | 19.73 | 6.10 | 19.73 | 42.72 |
| 12.75 | 19.23 | 9.96 | 19.23 | 42.83 |
| 13.74 | 15.76 | 11.97 | 15.96 | 42.76 |
| 9.21 | 20.09 | 8.19 | 20.09 | 42.41 |
| 15.57 | 18.86 | 3.52 | 18.86 | 43.18 |
| 11.90 | 19.24 | 6.30 | 19.24 | 42.72 |
| 10.28 | 16.94 | 13.43 | 19.24 | 42.36 |
| 12.18 | 18.86 | 7.37 | 16.96 | 42.73 |
| 12.39 | 18.56 | 7.74 | 18.86 | 42.74 |
| 16.75 | 16.80 | 6.42 | 18.56 | 43.22 |
| 12.92 | 18.00 | 8.22 | 18.11 | 42.78 |

Note: Last line represents the average for that column.

TABLE 13. OXIDE COMPOSITIONS PRESENT IN GMAW WITH C10 COVER GAS

| ALUMINUM | SILICON | TITANIUM | MANGANESE | OXYGEN |
|---|---|---|---|---|
| 16.48 | 16.49 | 7.38 | 16.49 | 43.17 |
| 10.83 | 15.49 | 15.65 | 15.71 | 42.31 |
| 12.49 | 15.15 | 14.66 | 15.15 | 42.56 |
| 17.17 | 17.76 | 3.97 | 17.76 | 43.33 |
| 16.60 | 18.37 | 3.36 | 18.37 | 43.29 |
| 15.55 | 15.95 | 9.53 | 15.95 | 43.02 |
| 14.74 | 18.60 | 5.00 | 18.60 | 43.06 |
| 16.13 | 16.30 | 8.16 | 16.30 | 43.11 |
| 17.58 | 17.58 | 3.88 | 17.58 | 43.38 |
| 14.61 | 17.63 | 7.13 | 17.63 | 42.99 |
| 12.18 | 18.37 | 8.37 | 16.37 | 42.71 |
| 17.46 | 17.55 | 4.08 | 17.55 | 43.36 |
| 16.83 | 16.85 | 6.24 | 16.85 | 43.24 |
| 15.56 | 15.57 | 10.32 | 15.57 | 43.00 |
| 17.04 | 17.04 | 5.60 | 17.04 | 43.28 |
| 15.54 | 19.39 | 2.47 | 19.39 | 43.21 |
| 11.62 | 22.27 | 0.97 | 22.28 | 42.85 |
| 12.42 | 17.25 | 10.40 | 17.25 | 42.67 |
| 12.01 | 18.41 | 8.48 | 18.41 | 42.69 |
| 14.96 | 19.44 | 3.02 | 19.44 | 43.14 |
| 14.89 | 17.57 | 6.93 | 17.48 | 43.02 |

Note: Last line represents the average for the column.

TABLE 14. AVERAGE OXIDE COMPOSITION FOR EACH WELD

| COVER GAS | Al | Si | Ti | Mn | O |
|---|---|---|---|---|---|
| 100% Ar | 12.77 | 19.22 | 6.68 | 30.14 | 38.56 |
| M-2 | 12.04 | 17.21 | 11.99 | 18.50 | 41.50 |
| MIDPOINT | 11.71 | 17.53 | 7.80 | 24.04 | 40.96 |
| C-5 | 11.55 | 18.16 | 8.96 | 18.77 | 42.44 |
| M-4 | 15.59 | 18.03 | 8.25 | 19.84 | 42.30 |
| C10/M4 | 12.92 | 18.00 | 8.22 | 18.11 | 42.78 |
| C-10 | 14.89 | 17.57 | 6.93 | 17.48 | 43.02 |

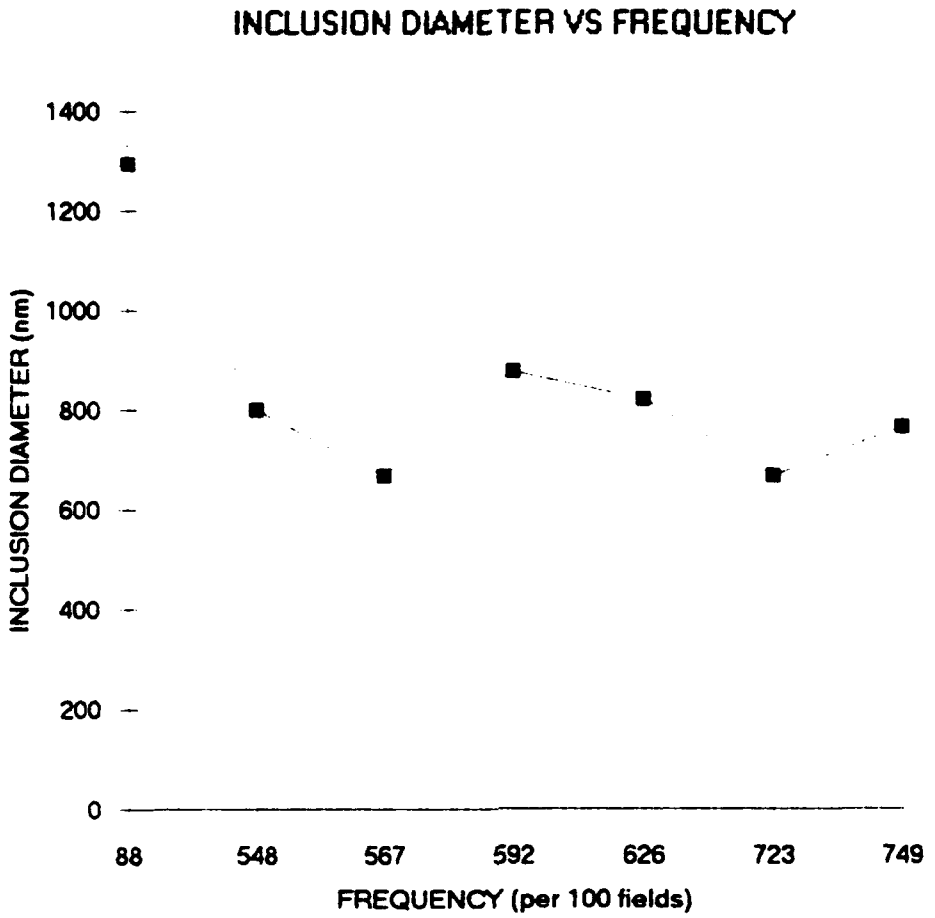


Figure 18. Chart representing the number of inclusions versus inclusion diameter.

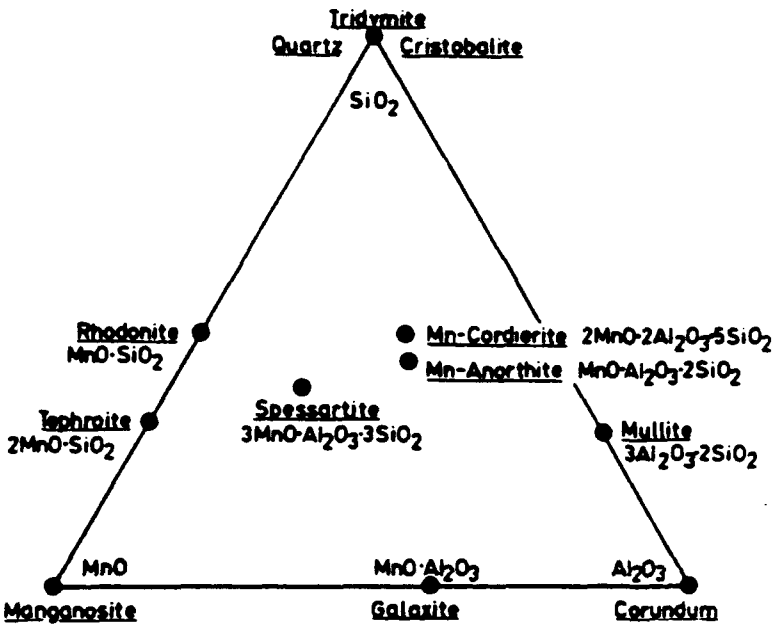


Figure 19. Schematic representation of the $MnO-SiO_2-Al_2O_3$ system. (Kiessling, 1978)

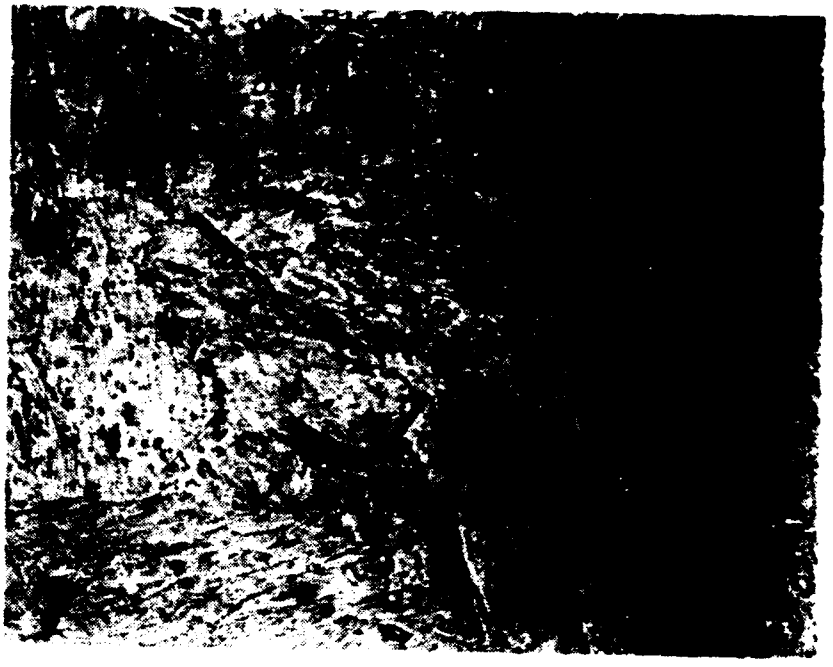

Figure 20. Optical micrograph of the etched weld (100% Argon cover gas). (400x)

Figure 21. Optical micrograph of the etched weld (M4 cover gas). (400x)

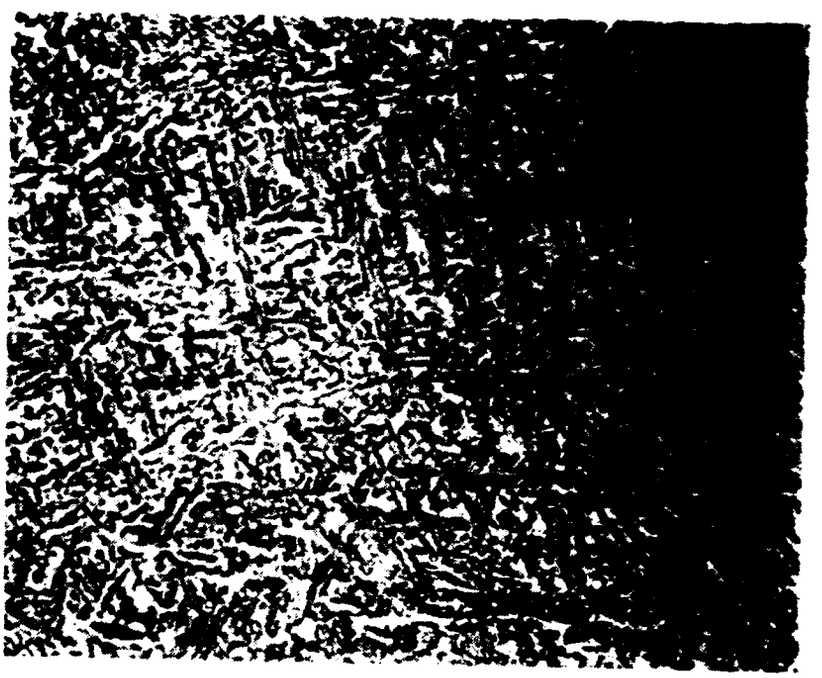

Figure 22. Optical micrograph of the etched weld (C10 cover gas). (400x)

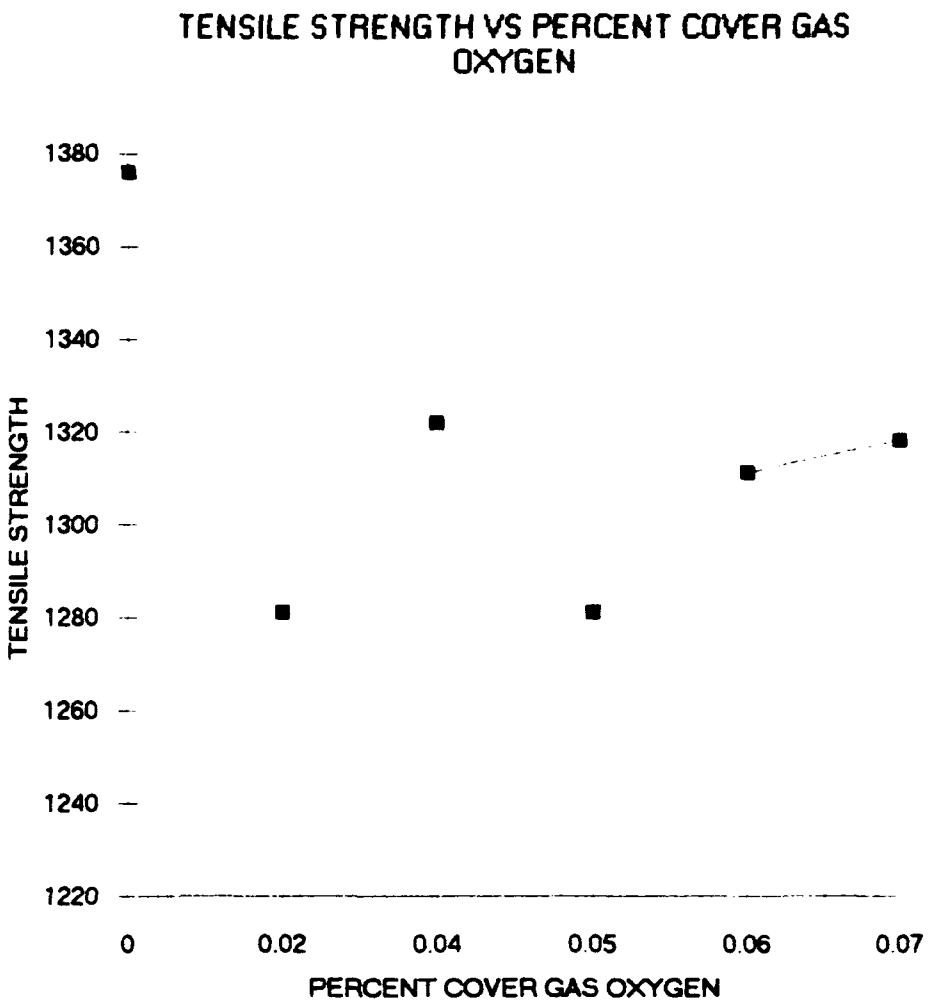


Figure 23. Line chart representing the decrease in calculated tensile strength versus the percent cover gas oxygen.

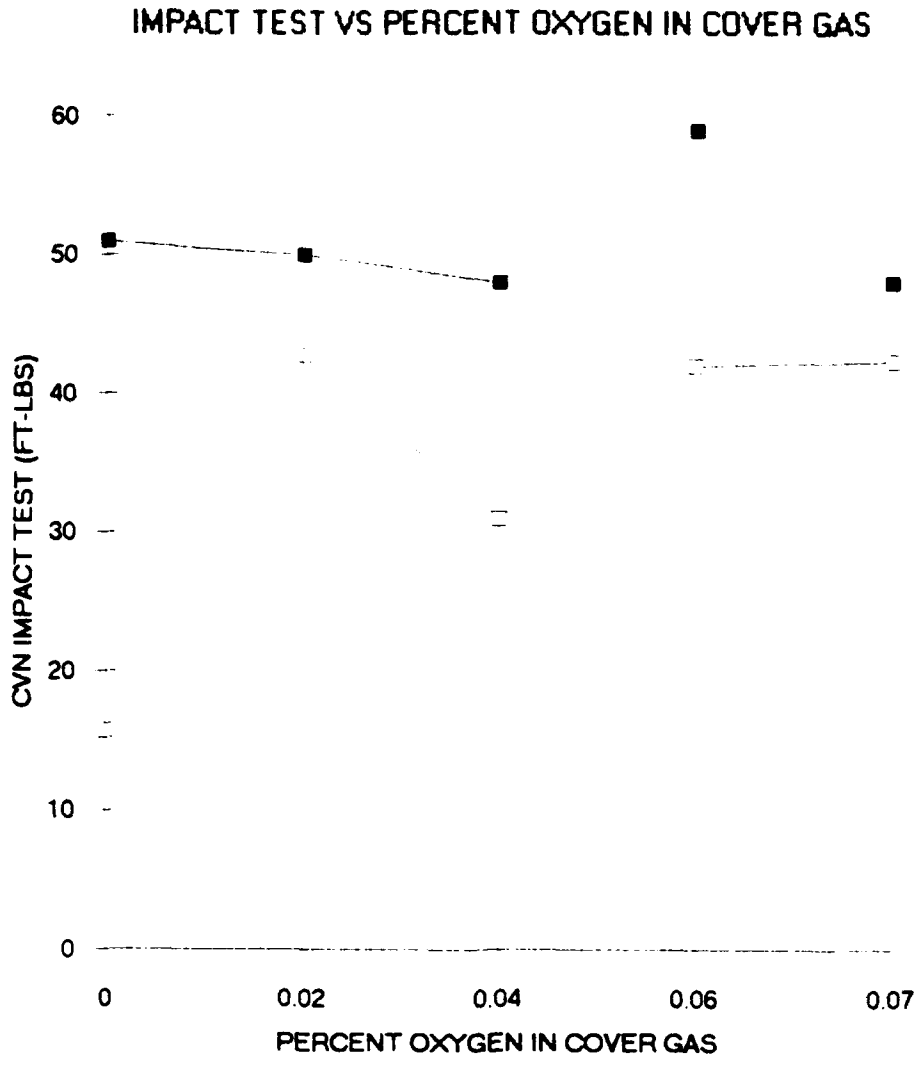


Figure 24. Line chart representing the Charpy impact results for zero degree Fahrenheit (upper line) and -60 degree Fahrenheit (lower line) versus percent cover gas oxygen.

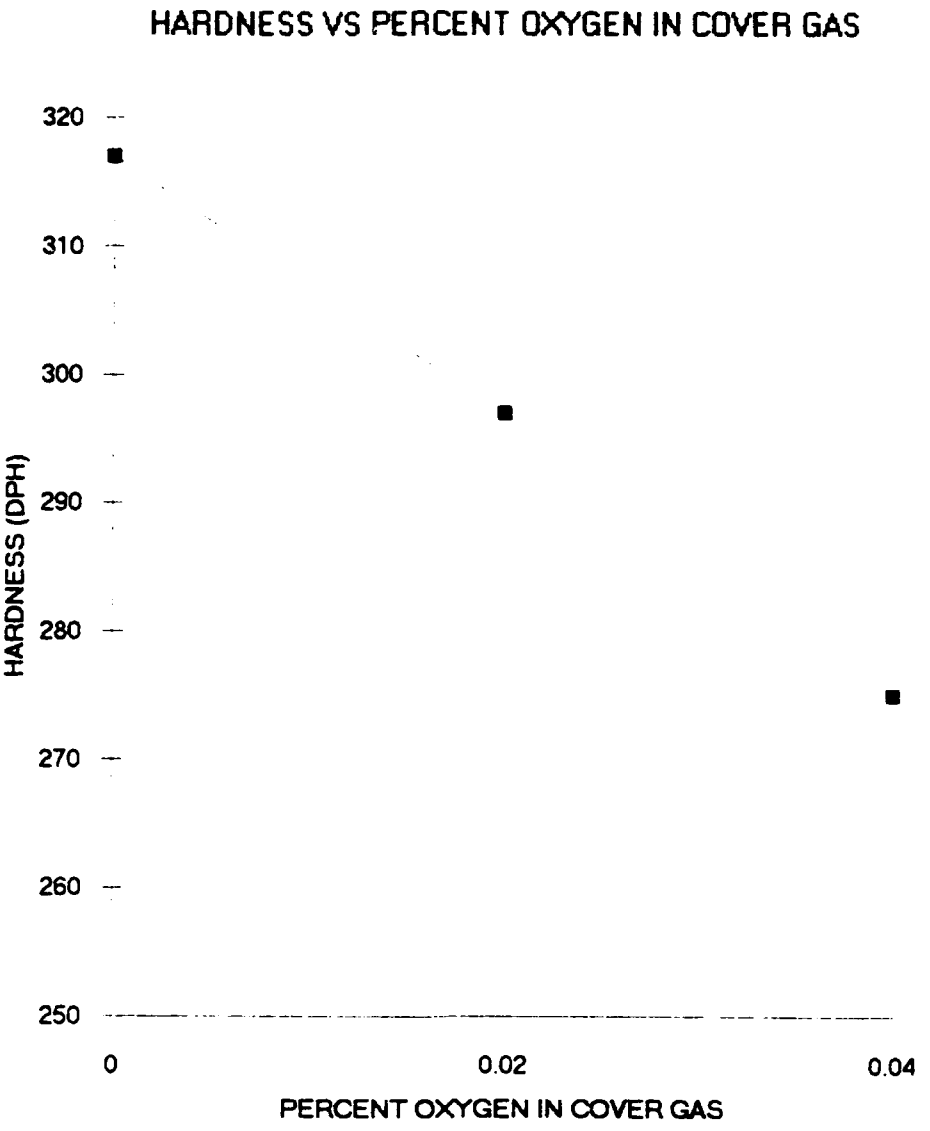


Figure 25. Line chart representing diamond point hardness versus M2 and M4 cover gases.

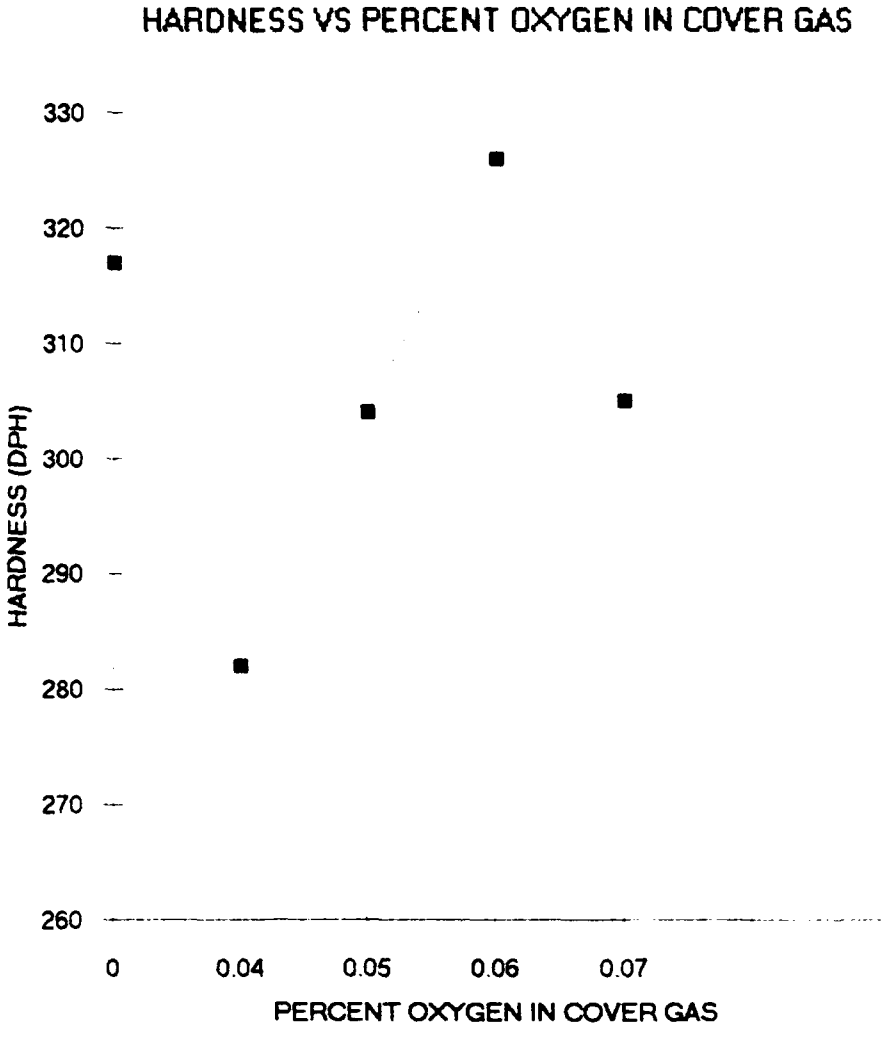


Figure 26. Line chart representing diamond point hardness versus midpoint, C5, C10/M4, and C10 cover gases.

## LIST OF REFERENCES


Czyryca, Earnest J., R.E. Link, R.J. Wong, D.A. Aylor, T.W. Montemarano and J.P. Gudas PhD, Development and Certification of HSLA-100 Steel for Naval Ship Construction, pp. 64-65, Naval Engineers Journal, May 1990.

Ellis, D., The Effects of Titanium Inclusions on HY-80 GMA Weld Deposits, p. 260, Master's Thesis, Naval Postgraduate School, Monterey, CA, December 1990.

Francis, R.E.,The Effect of Shield Gas Oxygen Activity on the Ferrite Content and Morphology of Gas Metal Arc Welded High Strength Low Alloy Steel, pp. 55-90, Master's Thesis, Colorado School of Mines, Golden, CO, 1984.

Hertzberg, R.W.,Deformation and Fracture Mechanics of Engineering Materials, pp. 370-390, 3rd ed., John Wiley and Sons, Inc., 1989.

Kiessling, R., Lange, N.,Non-metallic Inclusions in Steel, pp. 8-66, The Metal Society, London, 1978.

Kuo, S., Welding Metallurgy, pp. 16-17, John Wiley and Sons, New York, 1987.

Lancaster, J.F., Metallurgy of Welding, pp. 148-152, 4th ed., Allen and Unwin, London, 1987.

Mattes, V., Microstructure and Mechanical Properties of HSLA-100 Steel, p. 9, Master's Thesis, Naval Postgraduate School, Monterey, CA, December 1990.

Pickering, F.B.,Physical Metallurgy and the Design of Steels, p. 106, Applied Science Publishers LTD, London, 1978.

Olson, D.L., R. Dixon, A.L. Liby, A.L.,Welding Theory and Practice, pp. 123-129, Vol. 8, Elsevier Science Publishers, 1990.

Suka, A., Microstructure and Mechanical Properties of High Coppered HSLA-100 Steel in 2-Inch Plate Form, pp. 9-11, Master's Thesis, Naval Postgraduate School, Monterey, CA, June 1992.

Wilson, A.D., and others, Properties and Microstructure on Fracture Toughness of a High-Strength Low-Alloy Steel, pp. 60-290, Metallurgical Transactions A, Vol. 14A, October 1983.

Winters, H.A., A Study of the Microstructual Basis for the Strength and Toughness Properties of As-Quenched and Tempered High Copper HSLA-100 Steel, Master's Thesis, Naval Postgraduate School, Monterey, CA, December 1991.

## INITIAL DISTRIBUTION LIST

| | | No. Copies |
|---|---|---|
| 1. | Defense Technical Information Center<br>Cameron Station<br>Alexandria VA 22304-6145 | 2 |
| 2. | Library, Code 052<br>Naval Postgraduate School<br>Monterey CA 93943-5002 | 2 |
| 3. | Department Chairman, Code ME/Kk<br>Department of Mechanical Engineering<br>Naval Postgraduate School<br>Monterey, CA 93943-5000 | 1 |
| 4. | Naval Engineering Curricular Office, Code NE<br>Naval Postgraduate School<br>Monterey, CA 93943-5000 | 1 |
| 5. | Dr. Alan G. Fox, Code ME/Fo<br>Department of Mechanical Engineering<br>Naval Postgraduate School<br>Monterey, CA 93943-5000 | 2 |
| 6. | Lt. Ricky A. Seraiva<br>1330 Tulane Rd.<br>Wilmington, DE 19803 | 2 |
| 7. | Dr. M.G. Vassilaros, Code 2814<br>Annapolis Detachment, Carderock Division<br>Naval Surface Warfare Center (NSWC)<br>Annapolis, MD 21402 | 1 |